

EUROPEAN ORGANISATION FOR NUCLEAR RESEARCH (CERN)



Submitted to: JHEP



CERN-PH-2016-085
9th October 2018

Measurement of the relative width difference of the B^0 - \bar{B}^0 system with the ATLAS detector

The ATLAS Collaboration

Abstract

This paper presents the measurement of the relative width difference $\Delta\Gamma_d/\Gamma_d$ of the B^0 - \bar{B}^0 system using the data collected by the ATLAS experiment at the LHC in pp collisions at $\sqrt{s} = 7$ TeV and $\sqrt{s} = 8$ TeV and corresponding to an integrated luminosity of 25.2 fb^{-1} . The value of $\Delta\Gamma_d/\Gamma_d$ is obtained by comparing the decay-time distributions of $B^0 \rightarrow J/\psi K_S$ and $B^0 \rightarrow J/\psi K^{*0}(892)$ decays. The result is $\Delta\Gamma_d/\Gamma_d = (-0.1 \pm 1.1 \text{ (stat.)} \pm 0.9 \text{ (syst.)}) \times 10^{-2}$. Currently, this is the most precise single measurement of $\Delta\Gamma_d/\Gamma_d$. It agrees with the Standard Model prediction and the measurements by other experiments.

1 Introduction

The width difference $\Delta\Gamma_q$, where $q = d, s$, is one of the parameters describing the time evolution of the $B_q^0 - \bar{B}_q^0$ system. It is defined as $\Delta\Gamma_q \equiv \Gamma_q^L - \Gamma_q^H$, where Γ_q^L and Γ_q^H are the decay widths of the light and heavy B_q states, respectively. The relative value of $\Delta\Gamma_d/\Gamma_d$ is predicted in the Standard Model (SM) [1]:

$$\Delta\Gamma_d/\Gamma_d \text{ (SM)} = (0.42 \pm 0.08) \times 10^{-2}.$$

Here Γ_d is the total width of the B^0 meson defined as $\Gamma_d = \frac{1}{2}(\Gamma_d^L + \Gamma_d^H)$.

Measurements of $\Delta\Gamma_d$ have been performed by the BaBar [2], Belle [3], and LHCb [4] collaborations. The current world average value [5] is:

$$\Delta\Gamma_d/\Gamma_d \text{ (World average)} = (0.1 \pm 1.0) \times 10^{-2}.$$

The current experimental uncertainty in $\Delta\Gamma_d$ is too large to perform a stringent test of the SM prediction. In addition, independent measurements of other quantities do not constrain the value of $\Delta\Gamma_d$. It has been shown [6] that a relatively large variation of $\Delta\Gamma_d$ due to a possible new physics contribution would not contradict other existing SM tests. Therefore, an experimental measurement of $\Delta\Gamma_d$ with improved precision and its comparison to the SM prediction can provide an independent test of the underlying theory [7], complementary to other searches for new physics.

This paper presents the measurement of $\Delta\Gamma_d$ by the ATLAS experiment using Run 1 data collected in pp collisions at $\sqrt{s} = 7$ TeV in 2011 and at $\sqrt{s} = 8$ TeV in 2012. The total integrated luminosity used in this analysis is 4.9 fb^{-1} collected in 2011 and 20.3 fb^{-1} collected in 2012. The value of $\Delta\Gamma_d/\Gamma_d$ is obtained by comparing the decay time distributions of $B^0 \rightarrow J/\psi K_S$ and $B^0 \rightarrow J/\psi K^{*0}(892)$ decays.

2 Measurement method

The time evolution of the neutral $B_q^0 - \bar{B}_q^0$ system is described by the Schrödinger equation with Hamiltonian \mathbf{M}_q :

$$\begin{aligned} i\frac{d}{dt} \begin{pmatrix} B_q^0(t) \\ \bar{B}_q^0(t) \end{pmatrix} &= \mathbf{M}_q \begin{pmatrix} B_q^0(t) \\ \bar{B}_q^0(t) \end{pmatrix}, \\ \mathbf{M}_q &= \begin{pmatrix} m_q & m_q^{12} \\ (m_q^{12})^* & m_q \end{pmatrix} - \frac{i}{2} \begin{pmatrix} \Gamma_q & \Gamma_q^{12} \\ (\Gamma_q^{12})^* & \Gamma_q \end{pmatrix}. \end{aligned} \quad (1)$$

The non-diagonal elements of \mathbf{M}_q result from the transition $B_q^0 \leftrightarrow \bar{B}_q^0$ mediated by box diagrams and depend on the parameters of the CKM quark mixing matrix. Due to these non-diagonal elements, the B_q^0 meson propagates as a mixture of two physical mass eigenstates B_q^L and B_q^H :

$$|B_q^L\rangle = p|B_q^0\rangle + q|\bar{B}_q^0\rangle, \quad |B_q^H\rangle = p|B_q^0\rangle - q|\bar{B}_q^0\rangle. \quad (2)$$

Here p and q are complex numbers satisfying $|q|^2 + |p|^2 = 1$. B_q^L and B_q^H have distinct masses m_q^L, m_q^H and widths Γ_q^L, Γ_q^H . Assuming that $\Gamma_q^{12} \ll m_q^{12}$, the following relations hold:

$$\Delta m_q \equiv m_q^H - m_q^L = 2|m_q^{12}|, \quad (3)$$

$$\Delta\Gamma_q \equiv \Gamma_q^L - \Gamma_q^H = 2|\Gamma_q^{12}| \cos(\phi_q^{12}), \quad (4)$$

$$m_q \equiv \frac{1}{2}(m_q^L + m_q^H), \quad (5)$$

$$\Gamma_q \equiv \frac{1}{2}(\Gamma_q^L + \Gamma_q^H), \quad (6)$$

$$\phi_q^{12} \equiv \arg\left(-\frac{m_q^{12}}{\Gamma_q^{12}}\right). \quad (7)$$

The sign convention adopted in Eqs. (3) and (4) ensures that the values of Δm_q and $\Delta\Gamma_q$ are positive in the Standard Model.

The decay rates of the B_q^L and B_q^H mesons to a given final state f may be different. Therefore, the time dependence of the decay rate $B_q^0 \rightarrow f$ is sensitive to f . The time-dependent decay rate $\Gamma(B_q^0(t) \rightarrow f)$ is [8]:

$$\Gamma(B_q^0(t) \rightarrow f) \propto e^{-\Gamma_q t} \left[\cosh \frac{\Delta\Gamma_q t}{2} + A_{CP}^{\text{dir}} \cos(\Delta m_q t) + A_{\Delta\Gamma} \sinh \frac{\Delta\Gamma_q t}{2} + A_{CP}^{\text{mix}} \sin(\Delta m_q t) \right]. \quad (8)$$

Here t is the proper decay time of the B_q^0 meson. The parameters A_{CP}^{dir} , $A_{\Delta\Gamma}$ and A_{CP}^{mix} depend on the final state f . The abbreviations “dir” and “mix” stand for “direct” and “mixing”. By definition:

$$|A_{CP}^{\text{dir}}|^2 + |A_{\Delta\Gamma}|^2 + |A_{CP}^{\text{mix}}|^2 \equiv 1. \quad (9)$$

Assuming that the CP-violating phase ϕ_q^{12} is small, which is experimentally confirmed for both the B^0 and B_s^0 mesons [9], the time-dependent decay rate $\Gamma(\bar{B}_q^0(t) \rightarrow f)$ is:

$$\Gamma(\bar{B}_q^0(t) \rightarrow f) \propto e^{-\Gamma_q t} \left[\cosh \frac{\Delta\Gamma_q t}{2} - A_{CP}^{\text{dir}} \cos(\Delta m_q t) + A_{\Delta\Gamma} \sinh \frac{\Delta\Gamma_q t}{2} - A_{CP}^{\text{mix}} \sin(\Delta m_q t) \right]. \quad (10)$$

The parameters A_{CP}^{dir} , $A_{\Delta\Gamma}$ and A_{CP}^{mix} are theoretically well defined for flavour-specific final states and CP eigenstates [8]. For a flavour-specific final state f_{fs} , such that only the decay $B_q^0 \rightarrow f_{fs}$ is allowed while $\bar{A}_f = \langle f_{fs} | \bar{B}_q^0 \rangle = 0$, the parameters are:

$$A_{CP}^{\text{dir}} = 1, \quad A_{\Delta\Gamma} = 0, \quad A_{CP}^{\text{mix}} = 0. \quad (11)$$

For a flavour-specific final state \bar{f}_{fs} , such that $A_f = \langle \bar{f}_{fs} | B_q^0 \rangle = 0$, i.e. only the decay $\bar{B}_q^0 \rightarrow \bar{f}_{fs}$ is allowed, the parameters are:

$$A_{CP}^{\text{dir}} = -1, \quad A_{\Delta\Gamma} = 0, \quad A_{CP}^{\text{mix}} = 0. \quad (12)$$

For the B^0 decay to the CP eigenstate $J/\psi K_S$ the parameters are:

$$A_{CP}^{\text{dir}} = 0, \quad A_{\Delta\Gamma} = \cos(2\beta), \quad A_{CP}^{\text{mix}} = -\sin(2\beta). \quad (13)$$

Here β is the angle of the unitarity triangle of the CKM matrix:

$$\beta = \arg\left(-\frac{V_{cd}V_{cb}^*}{V_{td}V_{tb}^*}\right). \quad (14)$$

If the initial flavour of the B_q^0 meson is not tagged, the decay rates given by Eqs. (8) and (10) are added together. In this case, the production asymmetry A_P of the B_q^0 meson in pp collisions should be taken into account. This asymmetry is defined as:

$$A_P = \frac{\sigma(B_q^0) - \sigma(\bar{B}_q^0)}{\sigma(B_q^0) + \sigma(\bar{B}_q^0)}, \quad (15)$$

where σ denotes the production cross-section of the corresponding particle. Although b quarks are predominantly produced in $b\bar{b}$ pairs, which result in an equal number of b and \bar{b} quarks, the presence of a valence u quark in pp collisions leads to a small excess of B^+ mesons (quark content $\bar{b}u$) over B^- mesons ($b\bar{u}$) [10, 11]. Similarly, there is an excess of $B^0(\bar{b}d)$ mesons over $\bar{B}^0(b\bar{d})$ mesons due to the presence of a valence d quark. The larger number of B mesons than \bar{B} mesons is compensated for by the excess of b baryons over their corresponding anti-particles. In each case the excess is expected to be of the order of 1%. Only the LHCb experiment has measured A_P in pp collisions so far [12]. Their result is not directly applicable to the conditions of the ATLAS experiment because of the different ranges of pseudorapidities η and transverse momenta p_T of the detected B mesons. Therefore, a dedicated measurement of A_P is necessary. This measurement is presented in Section 6.

Taking into account the production asymmetry A_P and using Eqs. (8) and (10), the untagged time-dependent decay rate $\Gamma[t, f]$ to a final state f is:

$$\begin{aligned} \Gamma[t, f] &\equiv \sigma(B_q^0)\Gamma(B_q^0(t) \rightarrow f) + \sigma(\bar{B}_q^0)\Gamma(\bar{B}_q^0(t) \rightarrow f) \\ &\propto e^{-\Gamma_q t} \left[\cosh \frac{\Delta\Gamma_q t}{2} + A_P A_{CP}^{\text{dir}} \cos(\Delta m_q t) + A_{\Delta\Gamma} \sinh \frac{\Delta\Gamma_q t}{2} + A_P A_{CP}^{\text{mix}} \sin(\Delta m_q t) \right]. \end{aligned} \quad (16)$$

The width difference $\Delta\Gamma_q$ can be extracted from the decay time distribution of the decay $B_q^0(\bar{B}_q^0) \rightarrow f$ using Eqs. (11)–(16). Such a measurement employing a single final state f , although possible, would give poor precision for $\Delta\Gamma_q$. This is because $\Delta\Gamma_q \ll \Gamma_q$ and therefore the term $e^{-\Gamma_q t}$ dominates the decay time distribution. A more promising method [2] consists in obtaining $\Delta\Gamma_q$ from the ratio of the decay time distributions of two different decay modes of B_q , one of them being a CP eigenstate and the other a flavour-specific state. Using this ratio eliminates the dominant factor $e^{-\Gamma_q t}$ and leads to improved precision for $\Delta\Gamma_q$.

The measurement of $\Delta\Gamma_d$ presented in this paper employs the ratio of the CP eigenstate $J/\psi K_S$ and the flavour-specific states $J/\psi K^{*0}(892)$ and $J/\psi \bar{K}^{*0}(892)$. The $J/\psi K^{*0}$ and $J/\psi \bar{K}^{*0}$ states are added together and are denoted by $J/\psi K^{*0}$ throughout this paper, unless otherwise specified.

The decay rate $\Gamma[t, J/\psi K_S]$ is obtained from Eqs. (13)–(16):

$$\Gamma[t, J/\psi K_S] \propto e^{-\Gamma_{dt}} \left[\cosh \frac{\Delta\Gamma_{dt}}{2} + \cos(2\beta) \sinh \frac{\Delta\Gamma_{dt}}{2} - A_P \sin(2\beta) \sin(\Delta m_d t) \right]. \quad (17)$$

The expression for $\Gamma[t, J/\psi K^{*0}]$ is obtained from Eqs. (11), (12), and (16) by summing over the $J/\psi K^{*0}$ and $J/\psi \bar{K}^{*0}$ final states:

$$\Gamma[t, J/\psi K^{*0}] \propto e^{-\Gamma_{dt}} \cosh \frac{\Delta\Gamma_{dt}}{2}. \quad (18)$$

If the detection efficiencies of K^{*0} and \bar{K}^{*0} are different, the term proportional to A_P in Eq. (16) also contributes to Eq. (18). This contribution is multiplied by the relative difference in the detection efficiencies of K^{*0} and \bar{K}^{*0} mesons. Both of these factors are of the order of 10^{-2} , which is shown in Section 6. Therefore, the contribution of the term proportional to A_P is of the order of 10^{-4} and is neglected. Another contribution to Eq. (18) coming from CP violation in mixing is experimentally constrained to be less than 0.1% and is also neglected in this analysis.

The world average values of Γ_d , Δm_d and β are [5]:

$$1/\Gamma_d = (1.520 \pm 0.004) \times 10^{-12} \text{ s}, \quad (19)$$

$$\Delta m_d = (0.510 \pm 0.003) \times 10^{12} \text{ s}^{-1}, \quad (20)$$

$$\sin 2\beta = 0.682 \pm 0.019. \quad (21)$$

Their uncertainties produce a negligible impact on the measured value of $\Delta\Gamma_d$.

In this analysis, the proper decay length of the B^0 meson, $L_{\text{prop}}^B = ct$, is used in place of the proper decay time t . The procedure to measure L_{prop}^B is described in Section 5. The decay rates $\Gamma[L_{\text{prop}}^B, J/\psi K_S]$ and $\Gamma[L_{\text{prop}}^B, J/\psi K^{*0}]$ expressed as functions of L_{prop}^B are:

$$\Gamma[L_{\text{prop}}^B, J/\psi K_S] = \int_0^\infty G(L_{\text{prop}}^B - ct, J/\psi K_S) \Gamma[t, J/\psi K_S] dt, \quad (22)$$

$$\Gamma[L_{\text{prop}}^B, J/\psi K^{*0}] = \int_0^\infty G(L_{\text{prop}}^B - ct, J/\psi K^{*0}) \Gamma[t, J/\psi K^{*0}] dt. \quad (23)$$

Here $G(L_{\text{prop}}^B - ct, J/\psi K_S)$ and $G(L_{\text{prop}}^B - ct, J/\psi K^{*0})$ are the L_{prop}^B detector resolution functions for the $B^0 \rightarrow J/\psi K_S$ and $B^0 \rightarrow J/\psi K^{*0}$ channels, respectively. These functions are discussed in Section 5.

The width difference $\Delta\Gamma_d$ is obtained from the fit to the ratio $R(L_{\text{prop}}^B)$ of the distributions of the number of reconstructed $B^0 \rightarrow J/\psi K_S$ and $B^0 \rightarrow J/\psi K^{*0}$ candidates as a function of L_{prop}^B . The expected form of $R(L_{\text{prop}}^B)$ is obtained using Eqs. (22) and (23). The details of the fitting procedure are given in Section 8. Many experimental systematic uncertainties cancel in the ratio of the L_{prop}^B distributions, which improves the precision of the $\Delta\Gamma_d$ measurement. This is an important advantage of the method used in this analysis.

A similar method is used by the LHCb Collaboration [4], except that the value of $\Delta\Gamma_d$ is obtained from the difference of the partial decay widths of the $B^0 \rightarrow J/\psi K_S$ and $B^0 \rightarrow J/\psi K^{*0}$ decay modes and the production asymmetry $A_P(B^0)$ is not taken into account.

The J/ψ meson is reconstructed using the decay $J/\psi \rightarrow \mu^+ \mu^-$, which exploits a clean selection of J/ψ mesons and a highly efficient online trigger. The trigger efficiencies in the two B^0 decay channels are equal, apart from minor effects related to differences in the decay kinematics, as only the properties of the J/ψ meson are used to trigger the events. The K_S and K^{*0} mesons are reconstructed using the $K_S \rightarrow \pi^+ \pi^-$ and $K^{*0} \rightarrow K^+ \pi^- (\bar{K}^{*0} \rightarrow K^- \pi^+)$ decay modes. The details of this reconstruction are given in Section 4.

3 The ATLAS detector

The ATLAS experiment [13] uses a general-purpose detector consisting of an inner tracker, a calorimeter and a muon spectrometer. A brief outline of the components that are most relevant for this analysis is given below.

The ATLAS experiment uses a right-handed coordinate system with its origin at the nominal interaction point (IP) in the centre of the detector and the z -axis along the beam pipe. The x -axis points from the IP to the centre of the LHC ring, and the y -axis points upward. The inner detector (ID) surrounds the interaction point; it includes a silicon pixel detector (Pixel), a silicon microstrip detector (SCT) and a transition radiation tracker (TRT). The ID is immersed in an axial 2 T magnetic field. The ID covers the pseudorapidity range $|\eta| < 2.5$. The pseudorapidity is defined in terms of the polar angle θ as $\eta = -\ln \tan(\theta/2)$. The ID is enclosed by a calorimeter system containing electromagnetic and hadronic sections. The calorimeter is surrounded by a large muon spectrometer (MS) in an air-core toroidal magnet system. The MS contains a combination of monitored drift tubes (MDTs) and cathode strip chambers (CSCs), designed to provide precise position measurements in the bending plane in the range $|\eta| < 2.7$. In addition, resistive plate chambers (RPCs) and thin gap chambers (TGCs) with a coarse position resolution but a fast response time are used primarily to trigger muons in the ranges $|\eta| < 1.05$ and $1.05 < |\eta| < 2.4$, respectively. RPCs and TGCs are also used to provide position measurements in the non-bending plane and to improve the pattern recognition and track reconstruction. Momentum measurements in the MS are based on track segments formed in at least two of the three stations of the MDTs and the CSCs.

The ATLAS trigger system had three levels during Run 1: the hardware-based Level-1 trigger and the two-stage High Level Trigger (HLT), which comprises the Level-2 trigger and the Event Filter. At Level-1, the muon trigger searched for patterns of hits satisfying different transverse momentum thresholds using the RPCs and TGCs. The region-of-interest around these Level-1 hit patterns then served as a seed for the HLT muon reconstruction, in which dedicated algorithms were used to incorporate information from both the MS and the ID, achieving a position and momentum resolution close to that provided by the offline muon reconstruction.

4 Data sample and event selection

This analysis uses the full sample of pp collision data collected by the ATLAS detector in 2011 at $\sqrt{s} = 7$ TeV and in 2012 at $\sqrt{s} = 8$ TeV. After applying strict data quality criteria the integrated luminosity is 4.9 fb^{-1} for the 2011 sample and 20.3 fb^{-1} for the 2012 sample.

A set of dimuon trigger chains designed to select $J/\psi \rightarrow \mu^+ \mu^-$ decays is used [14, 15]. It includes numerous triggers with different muon p_T thresholds and additional topological and invariant mass requirements. Any dependence of the triggers on the proper decay time cancels to a good approximation in the ratio $R(L_{\text{prop}}^B)$ introduced in Section 2 because both the $B^0 \rightarrow J/\psi K_S$ and $B^0 \rightarrow J/\psi K^{*0}$ decays are selected with the same set of triggers.

For a given event, the primary vertex (PV) of the pp collision producing the B^0 meson is determined using good-quality tracks reconstructed in the ID. The average transverse position of the pp collisions (the beam spot) is used in this determination as a constraint. The beam spot is monitored continuously and is reconstructed at regular intervals using several thousand interactions collected from many events. The size of the beam spot for the 2012 data is $15 \mu\text{m}$ in the plane transverse to the beam direction. Due to the high LHC luminosity, each event containing a B^0 meson is accompanied by a large number of pile-up interactions, which occur at various z positions along the beam line. These background interactions produce several PV candidates. The selection of the primary vertex corresponding to the B^0 production point is described in Section 5.

The J/ψ candidates are reconstructed from pairs of oppositely charged muons with $p_T > 2.5$ GeV and $|\eta| < 2.4$. Their ID tracks are fitted to a common vertex. The χ^2 of the vertex fit must satisfy $\chi^2(J/\psi)/\text{NDF} < 16$, where NDF stands for the number of degrees of freedom and is equal to one in this case. The mass of the J/ψ candidate is required to be between 2.86 and 3.34 GeV.

The K_S candidates are reconstructed from pairs of oppositely charged particle tracks not used in the primary or pile-up vertex reconstruction. Each track is required to have at least one hit in either of the two silicon detectors. The transverse momenta of the tracks must be greater than 400 MeV and have $|\eta| < 2.5$. The pairs are fitted to a common vertex and kept if the $\chi^2(K_S)/\text{NDF} < 15$ (NDF = 1), and the projection of the distance between the J/ψ and K_S vertices along the K_S momentum in the transverse plane is less than 44 cm. The ratio of this projection to its uncertainty must be greater than 2. Two additional requirements are related to the point of closest approach of the K_S trajectory to the J/ψ vertex in the xy plane. The distance between this point and the position of the J/ψ decay vertex in the xy plane is required to be less than 2 mm. The difference in the z coordinates of these two points must be less than 10 mm. These requirements help to reduce the combinatorial background. The mass of the K_S candidate is required to be between 450 and 550 MeV.

The $B^0 \rightarrow J/\psi(\mu^+\mu^-) K_S(\pi^+\pi^-)$ candidates are constructed by refitting the four tracks of the J/ψ and K_S candidates. The muon tracks are constrained to intersect in a secondary vertex and their invariant mass is constrained to the nominal J/ψ mass [5]. The two pions from the K_S decay are constrained to originate from a tertiary vertex and their invariant mass is constrained to the nominal mass of the K_S meson [5]. The combined momentum of the refitted K_S decay tracks is required to point to the dimuon vertex. The fit has NDF = 6. The quality of the cascade vertex fit is ensured by the requirement $\chi^2(B^0) - \chi^2(J/\psi) < 25$. Finally, the transverse momentum of the B^0 is required to exceed 10 GeV.

For the selection of $B^0 \rightarrow J/\psi K^{*0}$ candidates, a J/ψ candidate and two additional oppositely charged particles are combined together. One particle is assigned the mass of the charged kaon and the other the mass of the charged pion. The transverse momentum of the kaon is required to exceed 800 MeV and the transverse momentum of the pion must be greater than 400 MeV. Both tracks must have $|\eta| < 2.5$. A vertex fit of the four selected tracks is performed where the invariant mass of the two muon tracks is constrained to the nominal J/ψ mass. All four tracks are constrained to originate from the same vertex. The fit has NDF = 6. The quality of the vertex fit is ensured by the requirement $\chi^2(B^0) - \chi^2(J/\psi) < 16$. The invariant mass of the $K\pi$ system is required to be between 850 and 950 MeV. This range is slightly shifted with respect to the world average value of the K^{*0} mass (895.81 ± 0.18 MeV) [5] to provide a better suppression of reflections from the $B_s \rightarrow J/\psi\phi$ decay. The transverse momentum of the $K\pi$ pair is required to exceed 2 GeV and the transverse momentum of the B^0 candidate is required to be greater than 10 GeV.

Particle identification of charged hadrons is not used in this analysis. Therefore, each pair of tracks is tested again with the assignments of the kaon and pion swapped. If both assignments satisfy the above selection criteria, the combination with the smaller deviation from the nominal K^{*0} mass is chosen. Section 6 gives more details about the number of such events. In this analysis the final states $J/\psi K^{*0}$ and $J/\psi \bar{K}^{*0}$ are not distinguished and the definition of the B^0 proper decay length discussed in Section 5 is not sensitive to the assignment of masses. Therefore, the misidentification between pion and kaon has a limited impact on the result of this analysis.

None of the presented selection criteria for the $J/\psi K_S$ and $J/\psi K^{*0}$ final states are applied relative to the primary interaction point, thus avoiding a bias in the decay time distribution of the B^0 candidates. Different groups of particles from the same event can be included in the $J/\psi K_S$ and $J/\psi K^{*0}$ samples. In

such cases, the additional candidates contribute to the combinatorial background and do not impact the signal yields.

For the measurement of $\Delta\Gamma_d$, the ratio $R(L_{\text{prop}}^B)$ built from the number of the reconstructed $B^0 \rightarrow J/\psi K_S$ and $B^0 \rightarrow J/\psi K^{*0}$ decays is used. In this ratio the dependence of the reconstruction efficiencies of the two final states on L_{prop}^B should be taken into account. A large part of this dependence, together with the associated uncertainties, cancels in $R(L_{\text{prop}}^B)$ because the number of final particles in both decay modes is the same and the procedure to measure L_{prop}^B described in Section 5 is similar in the two cases. Having similar selection criteria in the two channels also minimises the decay-time bias. Thus, the correction to the ratio $R(L_{\text{prop}}^B)$ is expected to be small. Still, it cannot be eliminated completely because the hadronic tracks in the $B^0 \rightarrow J/\psi K_S$ decay originate in a displaced $K_S \rightarrow \pi^+\pi^-$ vertex, whereas all four tracks in the $B^0 \rightarrow J/\psi K^{*0}$ decay originate in a single vertex. This difference between the two channels is the main source of the experimental bias in the ratio $R(L_{\text{prop}}^B)$, which can be evaluated only with Monte Carlo (MC) simulation. Using simulated events, the ratio of efficiencies to reconstruct $B^0 \rightarrow J/\psi K_S$ and $B^0 \rightarrow J/\psi K^{*0}$ decays, $R_{\text{eff}}(L_{\text{prop}}^B)$, is obtained as a function of L_{prop}^B .

The Monte Carlo samples are produced by simulating the production and decays of B^0 mesons using PYTHIA 6.1 [16] for the 7 TeV MC samples and with PYTHIA 8.1 [17] for the 8 TeV MC samples. In both cases, the underlying event, parton shower and hadronisation in the PYTHIA simulation are tuned with ATLAS data [18]. In all cases, the events are filtered at generator level by requiring two muons with $|\eta| < 2.5$ and transverse momenta exceeding 2.5 GeV for the 7 TeV samples and 3.5 GeV for the 8 TeV samples. The events are passed through a full simulation of the detector using the ATLAS simulation [19] based on Geant4 [20, 21] and processed with the same reconstruction algorithms as used for the data. All samples are produced with Monte Carlo configurations adjusted to properly account for different conditions during the two years of data-taking.

5 Proper decay length of the B^0 meson

The procedure adopted in this analysis to measure the proper decay length of the B^0 meson is explicitly designed to use the same input information for both the $B^0 \rightarrow J/\psi K_S$ and $B^0 \rightarrow J/\psi K^{*0}$ channels. The aim of this approach is to reduce the experimental bias in the ratio $R(L_{\text{prop}}^B)$. The origin of the B^0 meson coincides with the primary vertex of the pp collision. The tracks from the B^0 candidate are excluded in the measurement of the PV position. The position of the B^0 decay is determined by the J/ψ vertex, which is obtained from the vertex fit of the two muons. The residual impact of the additional particles from the B^0 decays is evaluated using MC simulation and is found to be small.

The proper decay length of the B^0 meson, L_{prop}^B , is determined in the xy plane of the detector because of the better precision compared to the measurement in three dimensions, strengthened by the small transverse size of the beam spot. A further advantage of measuring L_{prop}^B in the xy plane is the reduced dependence on pile-up interactions. The PV corresponding to the B^0 production point is selected from all reconstructed PVs as follows. For each PV candidate, the point of closest approach of the B^0 trajectory to the PV in the xy plane is determined and the difference δz of the z coordinates of these two points is measured. The candidate with the minimum absolute value of δz is selected as the B^0 production vertex. As with any other procedure of PV selection, this method is not ideal and occasionally a wrong PV is selected due to the resolution for the B^0 momentum direction. However, any selected PV should be close enough to the true B^0 production vertex because numerically $\delta z \sim O(1 \text{ mm})$ and both vertices are located

on the beam line, which has a slope of about 10^{-3} in both the xz and yz planes. The transverse size of the beam spot is about $15\ \mu\text{m}$ in both the x and y directions. Therefore, the distance between the true vertex and the selected vertex in the xy plane is expected to be much less than the precision of the decay length measurement, which is about $100\ \mu\text{m}$. Thus, the measurement of L_{prop}^B performed in the xy plane is not affected by a wrong selection of the PV in a small fraction of events.

For each reconstructed $B^0 \rightarrow J/\psi K_S$ or $B^0 \rightarrow J/\psi K^{*0}$ candidate, L_{prop}^B is measured using the projection of the B^0 decay length along the B^0 momentum in the plane transverse to the beam axis:

$$L_{\text{prop}}^B = \frac{(x^{J/\psi} - x^{\text{PV}})p_x^B + (y^{J/\psi} - y^{\text{PV}})p_y^B}{(p_T^B)^2} m_{B^0}. \quad (24)$$

Here $x^{J/\psi}, y^{J/\psi}$ are the coordinates of the J/ψ vertex; $x^{\text{PV}}, y^{\text{PV}}$ are the coordinates of the primary vertex; p_x^B, p_y^B are the x and y components of the momentum of the B^0 meson and $m_{B^0} = 5279.61\ \text{MeV}$ is its mass [5]. The resolution of L_{prop}^B is obtained from simulation and is parameterised by a double Gaussian function. It is found to be similar for the two decay modes due to the applied procedure for the L_{prop}^B measurement. The uncertainty in this resolution is propagated into the systematic uncertainty of the $\Delta\Gamma_d$ measurement as discussed in Section 9. To obtain the proper decay length distribution, the range of L_{prop}^B between -0.3 and $6\ \text{mm}$ is divided into ten bins defined in Table 1. The selected bin size is much larger than the expected L_{prop}^B resolution, which is about $34\ \mu\text{m}$. In each bin of L_{prop}^B , the number of $B^0 \rightarrow J/\psi K_S$ and $B^0 \rightarrow J/\psi K^{*0}$ decays are extracted from a binned log-likelihood fit to the corresponding mass distributions.

Bin number	1	2	3	4	5	6	7	8	9	10
Lower edge [mm]	-0.3	0.0	0.3	0.6	0.9	1.2	1.5	1.8	2.1	3.0
Upper edge [mm]	0.0	0.3	0.6	0.9	1.2	1.5	1.8	2.1	3.0	6.0

Table 1: Definition of the L_{prop}^B bins.

In this fit, the mass distributions are modelled by a sum of functions describing the signal and background components. For the $B^0 \rightarrow J/\psi K^{*0}$ channel, the signal function $f_s^{J/\psi K^{*0}}$ is defined as the sum of two Gaussian functions. The Gaussian functions are constrained to have the same mean. The background function $f_b^{J/\psi K^{*0}}$ is defined using an exponential function with a second-order polynomial as the exponent. The fit is first applied to the total sample to determine the mean and standard deviations of the two Gaussian functions and their relative fractions. For the fit in each L_{prop}^B bin, all parameters describing the signal, except the normalisation of $f_s^{J/\psi K^{*0}}$, are fixed to the values obtained in the fit of the total sample. It was verified in this analysis that fixing the parameters of the signal does not produce any bias in the result. The parameters of $f_b^{J/\psi K^{*0}}$ remain free.

The signal function for the $B^0 \rightarrow J/\psi K_S$ channel $f_s^{J/\psi K_S}$ is defined as the sum of two Gaussian functions. The background is modelled by the sum of two functions: $f_b^{J/\psi K_S} = f_b^c + f_b^{B_s}$. The combinatorial background function f_b^c is defined using an exponential function with a second-order polynomial as the exponent. The second function, $f_b^{B_s}$, accounts for the contribution from $B_s^0 \rightarrow J/\psi K_S$ decays and is defined as the sum of two Gaussian functions. The $B_s^0 \rightarrow J/\psi K_S$ contribution is visible in the mass distribution as a shoulder in the signal peak. Its fraction relative to the $B^0 \rightarrow J/\psi K_S$ signal is $\sim 1\%$. The

signal Gaussian functions are constrained to have the same mean. The relative fractions and standard deviations of the B_s^0 background Gaussian functions are parameterised to be the same as those of the signal Gaussian functions. The B_s^0 background Gaussian functions are also constrained to have the same mean. The mean of the B_s^0 background Gaussian functions is shifted relative to the mean of the signal Gaussian functions by the difference between the nominal masses of the B_s^0 and B^0 mesons (87.34 MeV) [5]. The fit is first applied to the total sample to determine the mean and standard deviations of the signal Gaussian functions and their relative fractions. For the fit in each L_{prop}^B bin, all parameters describing the signal, except the normalisation of $f_s^{J/\psi K_S}$, are fixed to the values obtained in the fit of the total sample. It was verified in this analysis that fixing the parameters of the signal does not produce any bias in the result. The parameters of $f_b^{B_s}$ are also fixed, except for the normalisation. All parameters of f_b^c remain free.

The separation of the $B^0 \rightarrow J/\psi K_S$ and $B_s^0 \rightarrow J/\psi K_S$ contributions is important for the $\Delta\Gamma_d$ measurement because the mean lifetimes of the B^0 and B_s^0 mesons decaying to this CP eigenstate are different. On the contrary, the separation of $B^0 \rightarrow J/\psi K^{*0}$ and $B_s^0 \rightarrow J/\psi K^{*0}$ decays is not necessary because the lifetimes of the B^0 and B_s^0 mesons decaying to this final state are equal to within 1% [5, 9]. Thus, the small ($\sim 1\%$) contribution of the $B_s^0 \rightarrow J/\psi K^{*0}$ decay does not have an impact on the $\Delta\Gamma_d$ measurement.

The fit ranges of the $J/\psi K_S$ and $J/\psi K^{*0}$ mass distributions are selected such that the background under the B^0 signal is smooth. The mass distribution $m(J/\psi K_S)$ contains a contribution from partially reconstructed $B \rightarrow J/\psi K_S \pi$ decays. This contribution has a threshold at $m(J/\psi K_S) \simeq 5130$ MeV. For this reason, the fit range $5160 < m(J/\psi K_S) < 5600$ MeV is selected. The corresponding contribution of $B \rightarrow J/\psi K^{*0} \pi$ decays is smaller. Therefore, the lower limit of the fit range of $m(J/\psi K^{*0})$ is selected at 5000 MeV. The impact of the selection of the fit range on the value of $\Delta\Gamma_d$ is included in the systematic uncertainty.

The total number of signal $B^0 \rightarrow J/\psi K_S$ decays obtained from the fit is $28\,170 \pm 250$ in the 2011 data set and $110\,830 \pm 520$ in the 2012 data set. For $B^0 \rightarrow J/\psi K^{*0}$ decays the corresponding numbers are $129\,200 \pm 900$ in the 2011 data set and $555\,800 \pm 1\,900$ in the 2012 data set. Figure 1 shows the fitted mass distribution of $B^0 \rightarrow J/\psi K_S$ candidates and $B^0 \rightarrow J/\psi K^{*0}$ candidates for $0.0 < L_{\text{prop}}^B < 0.3$ mm.

The ratio of the numbers of B^0 candidates in the two channels computed in each L_{prop}^B bin i gives the experimental ratio $R_{i,\text{uncor}}$ defined as:

$$R_{i,\text{uncor}} = \frac{N_i(J/\psi K_S)}{N_i(J/\psi K^{*0})}. \quad (25)$$

Here $N_i(J/\psi K_S)$ and $N_i(J/\psi K^{*0})$ are the numbers of events in a given bin i . This ratio has to be corrected by the ratio of the reconstruction efficiencies in the two channels as discussed in Section 7.

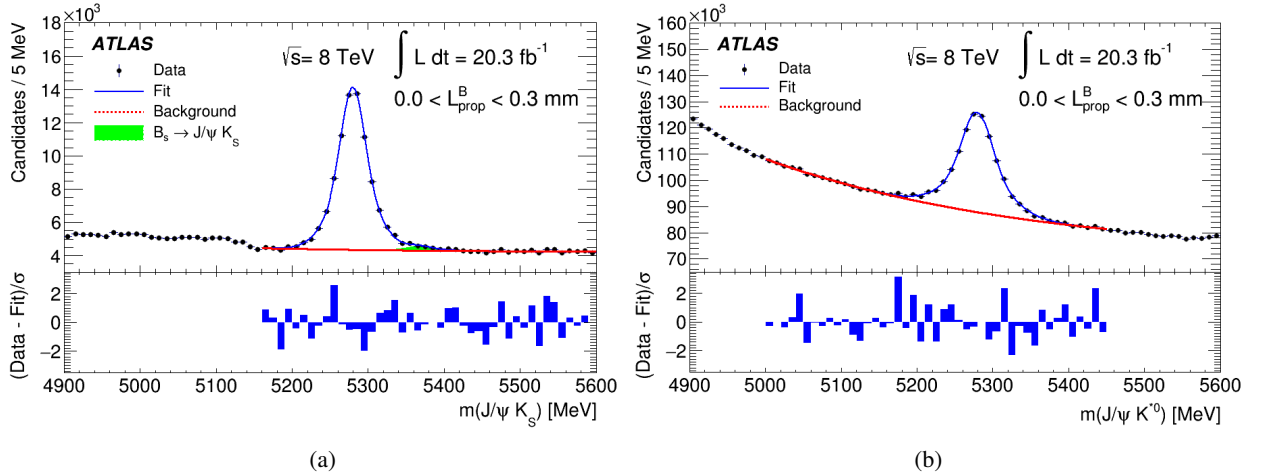


Figure 1: The invariant mass distributions for (a) $B^0 \rightarrow J/\psi K_S$ candidates and (b) $B^0 \rightarrow J/\psi K^{*0}$ candidates for the 2012 data sample for $0.0 < L_{\text{prop}}^B < 0.3$ mm. The full line shows the result of the fit to the function described in the text. The dashed line shows the combinatorial background contribution. The filled area in figure (a) shows the peaking background contribution from the $B_s^0 \rightarrow J/\psi K_S$ decay. The lower frame of each figure shows the difference between each data point and the fit at that point divided by the statistical uncertainty of the data point.

6 Production asymmetry of the B^0 meson

The production asymmetry A_P of the B^0 meson can be obtained from the time-dependent charge asymmetry of the flavour-specific $B^0 \rightarrow J/\psi K^{*0}$ decay. If the initial flavour of the B^0 meson is not determined, it follows from Eqs. (11), (12), and (16) that the time-dependent rate of the decay $B^0 \rightarrow J/\psi K^{*0}$ is equal to:

$$\Gamma[t, J/\psi K^{*0}] \propto e^{-\Gamma_d t} \left[\cosh \frac{\Delta \Gamma_d t}{2} + A_P \cos(\Delta m_d t) \right], \quad (26)$$

while the time-dependent rate of the decay $\bar{B}^0 \rightarrow J/\psi \bar{K}^{*0}$ is equal to:

$$\Gamma[t, J/\psi \bar{K}^{*0}] \propto e^{-\Gamma_d t} \left[\cosh \frac{\Delta \Gamma_d t}{2} - A_P \cos(\Delta m_d t) \right], \quad (27)$$

CP violation in mixing is predicted to be small in the SM and is omitted from these expressions.

The terms proportional to A_P in Eqs. (26) and (27) reflect the oscillating component of the $B^0 \rightarrow J/\psi K^{*0}$ decay. The corresponding charge asymmetry due to B^0 oscillations in bin i of L_{prop}^B , $A_{i,\text{osc}}$, is defined as:

$$A_{i,\text{osc}} \equiv \frac{\int_{L_i^{\min}}^{L_i^{\max}} \left(\int_0^{\infty} G(L_{\text{prop}}^B - ct, J/\psi K^{*0}) (\Gamma[t, J/\psi K^{*0}] - \Gamma[t, J/\psi \bar{K}^{*0}]) dt \right) dL_{\text{prop}}^B}{\int_{L_i^{\min}}^{L_i^{\max}} \left(\int_0^{\infty} G(L_{\text{prop}}^B - ct, J/\psi K^{*0}) (\Gamma[t, J/\psi K^{*0}] + \Gamma[t, J/\psi \bar{K}^{*0}]) dt \right) dL_{\text{prop}}^B}. \quad (28)$$

Here $G(L_{\text{prop}}^B - ct, J/\psi K^{*0})$ is the detector resolution of L_{prop}^B for the $B^0 \rightarrow J/\psi K^{*0}$ channel. The values of the lower and upper edges of bin i , L_i^{\min} and L_i^{\max} , are given in Table 1. Using Eqs. (26) and (27), $A_{i,\text{osc}}$

can be presented as:

$$A_{i,\text{osc}} = A_P \frac{\int_{L_i^{\min}}^{L_i^{\max}} \left(\int_0^\infty G(L_{\text{prop}}^B - ct, J/\psi K^{*0}) e^{-\Gamma_d t} \cos(\Delta m_d t) dt \right) dL_{\text{prop}}^B}{\int_{L_i^{\min}}^{L_i^{\max}} \left(\int_0^\infty G(L_{\text{prop}}^B - ct, J/\psi K^{*0}) e^{-\Gamma_d t} \cosh \frac{\Delta \Gamma_d t}{2} dt \right) dL_{\text{prop}}^B}. \quad (29)$$

In addition to B^0 oscillations, the asymmetry in the number of $J/\psi K^{*0}$ and $J/\psi \bar{K}^{*0}$ events is also caused by a detector-related asymmetry A_{det} due to differences in the reconstruction of positive and negative particles. The main source of A_{det} is the difference in the interaction cross-section of charged kaons with the detector material, which for momenta below 10 GeV is significantly larger for negative kaons [5]. Therefore, the observed number of $K^{*0} \rightarrow K^+ \pi^-$ decays is larger than that of $\bar{K}^{*0} \rightarrow K^- \pi^+$, resulting in a positive value of the detector asymmetry A_{det} . This effect is independent of the B^0 decay time.

The values of $A_{i,\text{osc}}$ and A_{det} are diluted by misidentification of the kaon and pion in the $B^0 \rightarrow J/\psi K^{*0}$ decay. The observed number of $J/\psi \bar{K}^{*0}$ events, $N(J/\psi \bar{K}^{*0})$, includes genuine $\bar{B}^0 \rightarrow J/\psi \bar{K}^{*0}$ and some $B^0 \rightarrow J/\psi K^{*0}$ decays. The latter decay contributes because of a wrong assignment of the kaon and pion masses to the two reconstructed charged particles, so that the decay $K^{*0} \rightarrow K^+ \pi^-$ is identified as a $\bar{K}^{*0} \rightarrow K^- \pi^+$. The mistag fraction W quantifies this wrong contribution to the $J/\psi \bar{K}^{*0}$ sample. It is defined as the fraction of true $B^0 \rightarrow J/\psi K^{*0}$ decays in $N(J/\psi \bar{K}^{*0})$. The mistag fraction does not depend on the B^0 decay time and is determined in simulation. The obtained value is:

$$W = 0.12 \pm 0.02. \quad (30)$$

The uncertainty of W is systematic. It takes into account possible variations of the MC simulation which describes B^0 production and decay. The simulation confirms that the mistag fraction is the same for $B^0 \rightarrow J/\psi K^{*0}$ and $\bar{B}^0 \rightarrow J/\psi \bar{K}^{*0}$ decays within the statistical uncertainty of 0.4% determined by the number of MC events. The systematic uncertainty of the difference of the mistag fraction of the $B^0 \rightarrow J/\psi K^{*0}$ and $\bar{B}^0 \rightarrow J/\psi \bar{K}^{*0}$ decays cancels to large extent. Therefore, the same value of W applies to candidates classified as $J/\psi K^{*0}$.

Using the above information, the expected charge asymmetry in bin i of L_{prop}^B , $A_{i,\text{exp}}$, can be expressed as:

$$A_{i,\text{exp}} = (A_{\text{det}} + A_{i,\text{osc}})(1 - 2W). \quad (31)$$

Here the factor $1 - 2W$ takes into account the contribution of wrongly identified B^0 decays, which is the same for both A_{det} and $A_{i,\text{osc}}$. The second-order terms proportional to $A_{\text{det}} A_P$ are of the order of 10^{-4} and are neglected in this expression.

The observed charge asymmetry, $A_{i,\text{obs}}$, is defined as:

$$A_{i,\text{obs}} \equiv \frac{N_i(J/\psi K^{*0}) - N_i(J/\psi \bar{K}^{*0})}{N_i(J/\psi K^{*0}) + N_i(J/\psi \bar{K}^{*0})}. \quad (32)$$

Figure 2 shows the asymmetry A_{obs} as a function of L_{prop}^B for the 2011 and 2012 samples combined together. The result of the fit to Eq. (31) is superimposed. The asymmetry A_P is obtained from a χ^2 minimisation:

$$\chi^2[A_{\text{det}}, A_P] = \sum_{i=2}^{10} \frac{(A_{i,\text{obs}} - A_{i,\text{exp}})^2}{\sigma_i^2}. \quad (33)$$

The free parameters in the fit are A_{det} and A_P . The values σ_i are the statistical uncertainties of $A_{i,\text{obs}}$. The fit has a χ^2 of 6.50 per seven degrees of freedom. The first bin of L_{prop}^B corresponds to a negative decay length due to the detector resolution. It is not included in this sum as it is affected more than the other data points by systematic uncertainties. Ignoring it has a negligible impact on the uncertainty of this measurement. The fit yields the following values for the asymmetries:

$$A_{\text{det}} = (+1.33 \pm 0.24 \pm 0.30) \times 10^{-2}. \quad (34)$$

$$A_P = (+0.25 \pm 0.48 \pm 0.05) \times 10^{-2}. \quad (35)$$

In these values the first uncertainty of A_P and A_{det} is statistical and the second is due to the uncertainties in the mistag fraction and in the deviations of $|q/p|$ from unity [5] (see Eq. (2)). The systematic uncertainty of A_{det} also contains a contribution from the possible difference between the mistag fractions of the $B^0 \rightarrow J/\psi K^{*0}$ and $\bar{B}^0 \rightarrow J/\psi \bar{K}^{*0}$ decays. The value of A_{det} is consistent with results from simulation of interactions in the detector. This measurement of the B^0 production asymmetry A_P for $p_T(B^0) > 10$ GeV and $|\eta(B^0)| < 2.5$ is consistent with zero. It is also consistent with the LHCb result $A_P = (-0.36 \pm 0.76 \pm 0.28) \times 10^{-2}$ [12] obtained for $4 < p_T(B^0) < 30$ GeV and $2.5 < \eta(B^0) < 4.0$. The measured value of A_P given in Eq. (35) is used for the extraction of the width difference $\Delta\Gamma_d$.

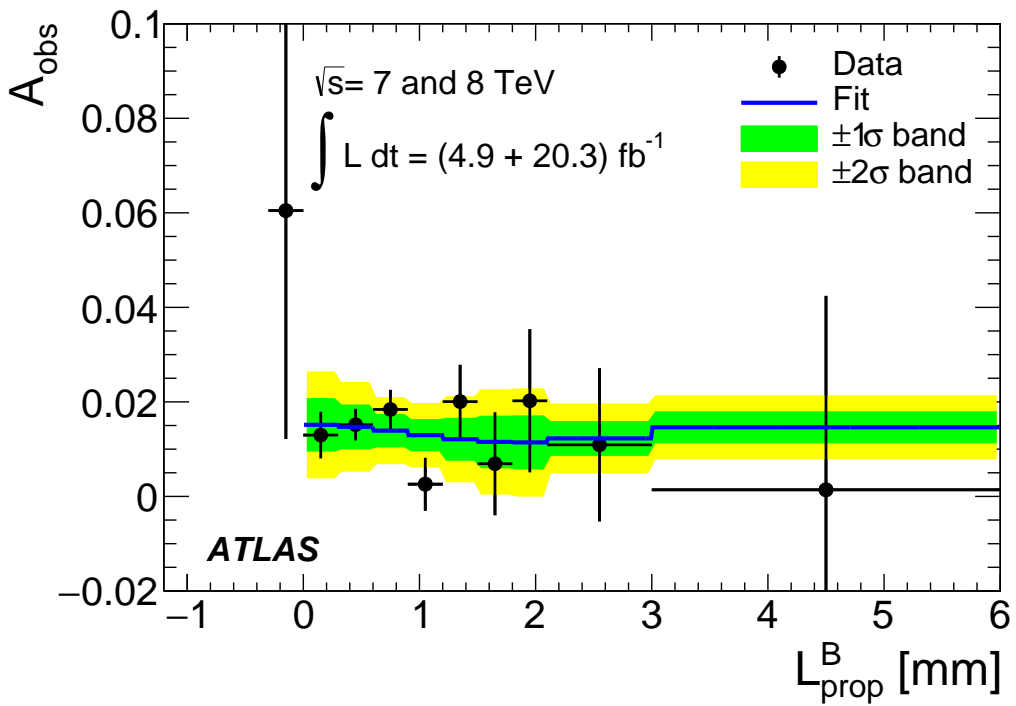


Figure 2: Observed charge asymmetry A_{obs} in $B^0 \rightarrow J/\psi K^{*0}$ decays measured as a function of the proper decay length of the B^0 meson (l_{prop}). The line shows the asymmetry A_{exp} obtained from fitting Eq. (31) to the data. The first point corresponding to negative proper decay length is not used in the fit. The error bands correspond to the combination of uncertainties obtained by the fit for the production asymmetry A_P and the detector asymmetry A_{det} .

7 Ratio of efficiencies

The ratio $R_{i,\text{uncor}}$ given by Eq. (25) is corrected by the ratio of efficiencies $R_{i,\text{eff}}$ computed in each L_{prop}^B bin i . It is defined as

$$R_{i,\text{eff}} \equiv \frac{\varepsilon_i(B^0 \rightarrow J/\psi K_S)}{\varepsilon_i(B^0 \rightarrow J/\psi K^{*0})}. \quad (36)$$

Here $\varepsilon_i(B^0 \rightarrow J/\psi K_S)$ and $\varepsilon_i(B^0 \rightarrow J/\psi K^{*0})$ are the efficiencies to reconstruct $B^0 \rightarrow J/\psi K_S$ and $B^0 \rightarrow J/\psi K^{*0}$ decays, respectively, in L_{prop}^B bin i . This ratio is determined using MC simulation. To obtain reliable values for this efficiency ratio, the kinematic properties of the simulated B^0 meson and the accompanying particles must be consistent with those in data. The comparison of several such properties, which can produce a sizeable impact on $R_{i,\text{eff}}$, reveal some differences between data and simulation. Those differences are corrected for by an appropriate re-weighting of the simulated events.

The properties taken into account include the transverse momentum and pseudorapidity of the B^0 meson and the average number of pile-up events. The ratio of the distributions of each specified variable in data and in simulation defines the corresponding weight. The resulting weight applied to the MC events is defined as the product of these three weights.

The normalisation of $R_{i,\text{eff}}$ after the re-weighting procedure is arbitrary since only the deviation of $R_{i,\text{eff}}$ from their average value can impact the measurement of $\Delta\Gamma_d$. This deviation is found to not exceed 5% for proper decay lengths up to 2 mm. Such a stability of $R_{i,\text{eff}}$ is a consequence of the chosen measurement procedure. This stability helps to reduce the systematic uncertainty of $\Delta\Gamma_d$ due to the uncertainty of the $R_{i,\text{eff}}$ value.

8 Fit of $\Delta\Gamma_d$

The obtained values of $R_{i,\text{eff}}$ are used to correct the observed ratio $R_{i,\text{uncor}}$ given by Eq. (25). The resulting ratio $R_{i,\text{cor}}$ is defined as:

$$R_{i,\text{cor}} = \frac{R_{i,\text{uncor}}}{R_{i,\text{eff}}}. \quad (37)$$

This ratio is shown in Figure 3. It is used to obtain $\Delta\Gamma_d/\Gamma_d$ by the following procedure. For each L_{prop}^B bin i defined in Table 1, the expected numbers of events in the $J/\psi K_S$ and $J/\psi K^{*0}$ channels are computed as:

$$N_i[\Delta\Gamma_d/\Gamma_d, J/\psi K_S] = C_1 \int_{L_i^{\min}}^{L_i^{\max}} \Gamma[L_{\text{prop}}^B, J/\psi K_S] dL_{\text{prop}}^B, \quad (38)$$

$$N_i[\Delta\Gamma_d/\Gamma_d, J/\psi K^{*0}] = C_2 \int_{L_i^{\min}}^{L_i^{\max}} \Gamma[L_{\text{prop}}^B, J/\psi K^{*0}] dL_{\text{prop}}^B. \quad (39)$$

The integration limits L_i^{\min} and L_i^{\max} for each bin i are given by the lower and upper bin edges in Table 1. C_1 and C_2 are arbitrary normalisation coefficients. The expressions for $\Gamma[L_{\text{prop}}^B, J/\psi K_S]$ and $\Gamma[L_{\text{prop}}^B, J/\psi K^{*0}]$ are given by Eqs. (22) and (23), respectively. The sensitivity to $\Delta\Gamma_d$ comes from $\Gamma[L_{\text{prop}}^B, J/\psi K_S]$ (see Eq. (17)) while $\Gamma[L_{\text{prop}}^B, J/\psi K^{*0}]$ provides the normalisation, which helps to reduce the systematic uncertainties.

The expected ratio of the decay rates in the two channels in each L_{prop}^B bin is:

$$R_{i,\text{exp}}[\Delta\Gamma_d/\Gamma_d] = \frac{N_i[\Delta\Gamma_d/\Gamma_d, J/\psi K_S]}{N_i[\Delta\Gamma_d/\Gamma_d, J/\psi K^{*0}]}.$$
 (40)

The relative width difference $\Delta\Gamma_d/\Gamma_d$ is obtained from a χ^2 minimisation:

$$\chi^2[\Delta\Gamma_d/\Gamma_d] = \sum_{i=2}^{10} \frac{(R_{i,\text{cor}} - R_{i,\text{exp}}[\Delta\Gamma_d/\Gamma_d])^2}{\sigma_i^2}.$$
 (41)

The values σ_i are the statistical uncertainties of $R_{i,\text{cor}}$. In the sum, the first bin of L_{prop}^B is not included as it corresponds to a negative decay length.

The free parameters in this minimisation are the overall normalisation and $\Delta\Gamma_d/\Gamma_d$. All other parameters describing the B^0 meson are fixed to their world average values. The fit is performed separately for the 2011 and 2012 samples because the systematic uncertainties for the two data samples are different. The result of the fit is shown in Figure 3. The χ^2 of the fit is 4.34 (NDF = 7) in the 2011 data set and 2.81 (NDF = 7) in the 2012 data set.

The fit yields

$$\Delta\Gamma_d/\Gamma_d = (-2.8 \pm 2.2 \text{ (stat.)} \pm 1.5 \text{ (MC stat.)}) \times 10^{-2} \quad (2011),$$
 (42)

$$\Delta\Gamma_d/\Gamma_d = (+0.8 \pm 1.3 \text{ (stat.)} \pm 0.5 \text{ (MC stat.)}) \times 10^{-2} \quad (2012).$$
 (43)

Here the uncertainties due to the data and MC statistics are given separately. The systematic uncertainties are discussed in Section 9.

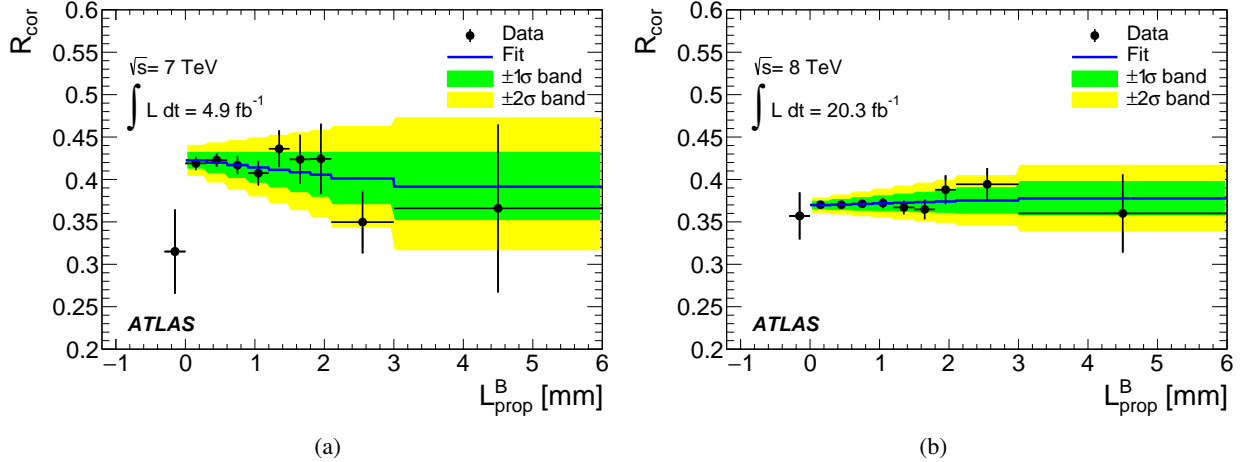


Figure 3: Efficiency-corrected ratio of the observed decay length distributions, $R_{\text{cor}}(L_{\text{prop}}^B)$ for (a) $\sqrt{s} = 7 \text{ TeV}$ and (b) $\sqrt{s} = 8 \text{ TeV}$ data sets. The normalisation of the two data sets is arbitrary. The full line shows the fit of $R_{\text{cor}}(L_{\text{prop}}^B)$ to R_{exp} given by Eq. (40). The error bands correspond to uncertainties in $\Delta\Gamma_d/\Gamma_d$ determined by the fit.

9 Systematic uncertainties

The relative B^0 width difference is extracted from the ratio of the L_{prop}^B distributions in the two B^0 decay modes, which are obtained using a similar procedure, the same type of information and in the same production environment. Therefore, the impact of many systematic uncertainties, such as the trigger selection, decay-time resolution or B^0 production properties, is negligible. However, some differences between the $B^0 \rightarrow J/\psi K_S$ and $B^0 \rightarrow J/\psi K^{*0}$ channels cannot be eliminated and the inaccuracy of their simulation results in systematic uncertainties, which are estimated in this section.

The mean proper decay length of the K_S meson is 26.8 mm. Since the p_T of the K_S meson can be high, some K_S mesons decay outside the inner detector and are lost. The probability of losing a K_S meson is higher for large B^0 decay time due to the reduction of the fiducial volume of the K_S decay. Thus, the displaced vertex of the K_S decay and the absence of such a vertex in the $K^{*0} \rightarrow K^+ \pi^-$ decay results in a decay-time dependence of R_{eff} defined in Eq. (36). Applying the correction given by Eq. (37) to R_{uncor} takes into account this dependence.

The test of the simulated K_S reconstruction is performed by comparing the distribution of the K_S decay length and the K_S pseudorapidity in data and simulation. This dedicated study shows that there is a residual difference between data and MC simulation in the distributions of the laboratory decay length of reconstructed K_S mesons projected along the K_S momentum in the transverse plane, $L_{xy}(K_S)$. It is caused by the remaining difference between the K_S momentum distributions in data and MC simulation. After applying an additional weight to the Monte Carlo events to correct for this difference a change in the value of $\Delta\Gamma_d/\Gamma_d$ of $\delta(\Delta\Gamma_d/\Gamma_d) = -0.21 \times 10^{-2}$ is obtained for the 2011 data set and $\delta(\Delta\Gamma_d/\Gamma_d) = -0.16 \times 10^{-2}$ for the 2012 data set. This difference is taken as the systematic uncertainty due to modelling of the $L_{xy}(K_S)$ dependence of the K_S reconstruction.

The same procedure is applied for the pseudorapidity distribution of the K_S meson, $\eta(K_S)$. The systematic uncertainty due to modelling of the $|\eta(K_S)|$ dependence of the K_S reconstruction is estimated by re-weighting the MC events to make the $|\eta(K_S)|$ distribution the same as in data. The observed changes are $\delta(\Delta\Gamma_d/\Gamma_d) = +0.14 \times 10^{-2}$ for the 2011 data set and $\delta(\Delta\Gamma_d/\Gamma_d) = -0.01 \times 10^{-2}$ for the 2012 data set.

The systematic uncertainty due to the choices made in the model used to fit the mass distributions can be estimated by considering different variations of the fit model. The range over which the $B^0 \rightarrow J/\psi K_S$ and $B^0 \rightarrow J/\psi K^{*0}$ mass fits are applied is varied and the measurement of $\Delta\Gamma_d/\Gamma_d$ is repeated for each variation. The systematic uncertainty is estimated by taking the difference between the values of $\Delta\Gamma_d/\Gamma_d$ obtained from the default fit and each of the varied fits. Variations $\delta(\Delta\Gamma_d/\Gamma_d) = -0.47 \times 10^{-2}$ and -0.30×10^{-2} are obtained for the 2011 data set in the $J/\psi K_S$ and $J/\psi K^{*0}$ channels, respectively. The changes for the 2012 data set are $\delta(\Delta\Gamma_d/\Gamma_d) = -0.59 \times 10^{-2}$ and -0.15×10^{-2} in the $J/\psi K_S$ and $J/\psi K^{*0}$ channels, respectively. These values are included as the systematic uncertainty from this source.

Additionally, the background function is changed from an exponential to a fourth-order polynomial and the systematic uncertainty due to the choice of background function is estimated from the difference between the value of $\Delta\Gamma_d/\Gamma_d$ from the default fit and the value from the fit using the polynomial background function. A change $\delta(\Delta\Gamma_d/\Gamma_d) = -0.16 \times 10^{-2}$ is obtained for the 2011 data set. The change for the 2012 data set is $\delta(\Delta\Gamma_d/\Gamma_d) = +0.09 \times 10^{-2}$.

In the fit of the number of $B^0 \rightarrow J/\psi K_S$ decays the contribution from the $B_s^0 \rightarrow J/\psi K_S$ is a free parameter of the fit. As a systematic uncertainty cross-check, the ratio of the yields of these two decays is fixed to be the same as that measured by the LHCb Collaboration [22]. The resulting change in the $\Delta\Gamma_d/\Gamma_d$ value

is $\delta(\Delta\Gamma_d/\Gamma_d) = -0.11 \times 10^{-2}$ for the 2011 data set and $\delta(\Delta\Gamma_d/\Gamma_d) = +0.08 \times 10^{-2}$ for the 2012 data set and is included as an additional source of systematic uncertainty.

The systematic uncertainty due to the resolution of L_{prop}^B is also considered. The average decay length resolution is $35 \mu\text{m}$ for $B_s^0 \rightarrow J/\psi K_S$ and $33 \mu\text{m}$ for $B^0 \rightarrow J/\psi K^{*0}$. In this analysis, separate resolution functions are used for the two channels. To test the sensitivity to the resolution, the measurement of $\Delta\Gamma_d/\Gamma_d$ is repeated by using the resolution of $J/\psi K^{*0}$ for both channels. A change in the value of $\Delta\Gamma_d/\Gamma_d$ of $\delta(\Delta\Gamma_d/\Gamma_d) = -0.29 \times 10^{-2}$ is obtained and is used as the systematic uncertainty from this source. It is found to be the same for the 2011 and 2012 data sets.

A toy MC sample is employed to identify any possible bias in the fitting procedure. In this toy MC sample, the expected number of $J/\psi K_S$ and $J/\psi K^{*0}$ candidates in each bin of L_{prop}^B is determined according to the analytic functions given by Eqs. (17) and (18), respectively, and a value of $\Delta\Gamma_d/\Gamma_d = 0.42 \times 10^{-2}$ corresponding to the SM expectation [1]. Using these expected numbers of candidates as the mean values, the number of candidates in both channels is randomly generated in each L_{prop}^B bin with an uncertainty corresponding to that obtained in data. The ratio of the obtained distributions is then fitted using the method described in Section 8. The procedure is repeated 10 000 times giving a bias in the mean fitted value $\delta(\Delta\Gamma_d/\Gamma_d) = +0.07 \times 10^{-2}$. This value is used as the systematic uncertainty due to the fitting procedure and it is taken to be the same for the 2011 and 2012 data sets.

The impact of the uncertainty of the B^0 production asymmetry is $\delta(\Delta\Gamma_d/\Gamma_d) = 0.01 \times 10^{-2}$ for both the 2011 and 2012 data sets.

The systematic uncertainty from the number of events in the MC samples corresponds to an uncertainty of $\delta(\Delta\Gamma_d/\Gamma_d) = 1.54 \times 10^{-2}$ for the 2011 data set and $\delta(\Delta\Gamma_d/\Gamma_d) = 0.45 \times 10^{-2}$ for the 2012 data set.

Table 2 gives a summary of the estimated systematic uncertainties. All of the quantified systematic uncertainties are symmetrized.

In addition to the estimate of the systematic uncertainty, several cross-checks are performed. Some of the selection cuts described in Section 6 are modified and the corresponding changes in the $\Delta\Gamma_d/\Gamma_d$ value are assessed. In particular, the transverse momenta of the charged pions from the K_S decay and the charged pion from the K^{*0} decay are required to be greater than 500 MeV, rather than 400 MeV. Also, the transverse momentum of the charged kaon from the K^{*0} is required to be greater than 1 GeV, rather than 800 MeV. Additionally, the transverse momentum of the B^0 meson is required to be less than 60 GeV. In all cases, the change of the measured value of $\Delta\Gamma_d$ is consistent with fluctuations due to the reduced number of events.

Furthermore, a number of consistency checks related to the description of the experimental conditions in simulation are performed. Most notably, the MC description of the spread of the z position of the primary vertex, the angular distributions of the B^0 decay products, and the trigger rates are studied in detail. In all cases, the residual differences between data and MC simulation do not impact the measured value of $\Delta\Gamma_d$.

Source	$\delta(\Delta\Gamma_d/\Gamma_d)$, 2011	$\delta(\Delta\Gamma_d/\Gamma_d)$, 2012
K_S decay length	0.21×10^{-2}	0.16×10^{-2}
K_S pseudorapidity	0.14×10^{-2}	0.01×10^{-2}
$B^0 \rightarrow J/\psi K_S$ mass range	0.47×10^{-2}	0.59×10^{-2}
$B^0 \rightarrow J/\psi K^{*0}$ mass range	0.30×10^{-2}	0.15×10^{-2}
Background description	0.16×10^{-2}	0.09×10^{-2}
$B_s^0 \rightarrow J/\psi K_S$ contribution	0.11×10^{-2}	0.08×10^{-2}
L_{prop}^B resolution	0.29×10^{-2}	0.29×10^{-2}
Fit bias (Toy MC)	0.07×10^{-2}	0.07×10^{-2}
B^0 production asymmetry	0.01×10^{-2}	0.01×10^{-2}
MC sample	1.54×10^{-2}	0.45×10^{-2}
Total uncertainty	1.69×10^{-2}	0.84×10^{-2}

Table 2: Sources of systematic uncertainty in the $\Delta\Gamma_d/\Gamma_d$ measurement and their values for the 2011 and 2012 data sets.

10 Results

Using the measurements of $\Delta\Gamma_d/\Gamma_d$ given in Eqs. (42) and (43) and the study of systematic uncertainties presented in Section 9, the following measurements are obtained:

$$\begin{aligned}\Delta\Gamma_d/\Gamma_d &= (-2.8 \pm 2.2 \text{ (stat.)} \pm 1.7 \text{ (syst.)}) \times 10^{-2} \quad (2011), \\ \Delta\Gamma_d/\Gamma_d &= (+0.8 \pm 1.3 \text{ (stat.)} \pm 0.8 \text{ (syst.)}) \times 10^{-2} \quad (2012).\end{aligned}$$

In the combination of these measurements, the correlations of different sources of systematic uncertainty between the two years are taken into account. The systematic uncertainties due to the background description and the size of the MC samples are assumed to be uncorrelated. All other sources of systematic uncertainty are taken to be fully correlated. The combination is done using the χ^2 method. The χ^2 function includes the correlation terms of the different components of the uncertainty as specified above. The combined result for the data collected by the ATLAS experiment in Run 1 is:

$$\Delta\Gamma_d/\Gamma_d = (-0.1 \pm 1.1 \text{ (stat.)} \pm 0.9 \text{ (syst.)}) \times 10^{-2}.$$

It is currently the most precise single measurement of this quantity. It agrees well with the SM prediction [1] and is consistent with other measurements of this quantity [2–4]. It also agrees with the indirect measurement by the D0 Collaboration [23].

11 Conclusions

The measurement of the relative width difference $\Delta\Gamma_d/\Gamma_d$ of the $B^0-\bar{B}^0$ system is performed using the data collected by the ATLAS experiment at the LHC in pp collisions at $\sqrt{s} = 7$ TeV and $\sqrt{s} = 8$ TeV and corresponding to an integrated luminosity of 25.2 fb^{-1} . The value of $\Delta\Gamma_d/\Gamma_d$ is obtained by comparing the decay time distributions of $B^0 \rightarrow J/\psi K_S$ and $B^0 \rightarrow J/\psi K^{*0}(892)$ decays. The result is

$$\Delta\Gamma_d/\Gamma_d = (-0.1 \pm 1.1 \text{ (stat.)} \pm 0.9 \text{ (syst.)}) \times 10^{-2}.$$

Currently, this is the most precise single measurement of $\Delta\Gamma_d/\Gamma_d$. It agrees with the Standard Model prediction and the measurements by other experiments.

The production asymmetry of the B^0 meson with $p_T(B^0) > 10$ GeV and $|\eta(B^0)| < 2.5$ is found to be

$$A_P(B^0) = (+0.25 \pm 0.48 \pm 0.05) \times 10^{-2}.$$

The value of $A_P(B^0)$ is consistent with the measurement of the LHCb Collaboration performed in the $2.5 < \eta(B^0) < 4.0$ and $4 < p_T(B^0) < 30$ GeV range.

Acknowledgements

We thank CERN for the very successful operation of the LHC, as well as the support staff from our institutions without whom ATLAS could not be operated efficiently.

We acknowledge the support of ANPCyT, Argentina; YerPhI, Armenia; ARC, Australia; BMWFW and FWF, Austria; ANAS, Azerbaijan; SSTC, Belarus; CNPq and FAPESP, Brazil; NSERC, NRC and CFI, Canada; CERN; CONICYT, Chile; CAS, MOST and NSFC, China; COLCIENCIAS, Colombia; MSMT CR, MPO CR and VSC CR, Czech Republic; DNRF and DNSRC, Denmark; IN2P3-CNRS, CEA-DSM/IRFU, France; GNSF, Georgia; BMBF, HGF, and MPG, Germany; GSRT, Greece; RGC, Hong Kong SAR, China; ISF, I-CORE and Benoziyo Center, Israel; INFN, Italy; MEXT and JSPS, Japan; CNRST, Morocco; FOM and NWO, Netherlands; RCN, Norway; MNiSW and NCN, Poland; FCT, Portugal; MNE/IFA, Romania; MES of Russia and NRC KI, Russian Federation; JINR; MESTD, Serbia; MSSR, Slovakia; ARRS and MIZŠ, Slovenia; DST/NRF, South Africa; MINECO, Spain; SRC and Wallenberg Foundation, Sweden; SERI, SNSF and Cantons of Bern and Geneva, Switzerland; MOST, Taiwan; TAEK, Turkey; STFC, United Kingdom; DOE and NSF, United States of America. In addition, individual groups and members have received support from BCKDF, the Canada Council, CANARIE, CRC, Compute Canada, FQRNT, and the Ontario Innovation Trust, Canada; EPLANET, ERC, FP7, Horizon 2020 and Marie Skłodowska-Curie Actions, European Union; Investissements d’Avenir Labex and Idex, ANR, Région Auvergne and Fondation Partager le Savoir, France; DFG and AvH Foundation, Germany; Herakleitos, Thales and Aristeia programmes co-financed by EU-ESF and the Greek NSRF; BSF, GIF and Minerva, Israel; BRF, Norway; Generalitat de Catalunya, Generalitat Valenciana, Spain; the Royal Society and Leverhulme Trust, United Kingdom.

The crucial computing support from all WLCG partners is acknowledged gratefully, in particular from CERN and the ATLAS Tier-1 facilities at TRIUMF (Canada), NDGF (Denmark, Norway, Sweden), CC-IN2P3 (France), KIT/GridKA (Germany), INFN-CNAF (Italy), NL-T1 (Netherlands), PIC (Spain), ASGC (Taiwan), RAL (UK) and BNL (USA) and in the Tier-2 facilities worldwide.

References

- [1] A. Lenz and U. Nierste, ‘Numerical Updates of Lifetimes and Mixing Parameters of B Mesons’, *CKM unitarity triangle. Proceedings, 6th International Workshop, CKM 2010, Warwick, UK, September 6-10, 2010*, 2011, arXiv:[1102.4274 \[hep-ph\]](https://arxiv.org/abs/1102.4274).

- [2] BaBar Collaboration, B. Aubert et al., *Limits on the decay rate difference of neutral-B mesons and on CP, T, and CPT violation in $B^0\bar{B}^0$ oscillations*, *Phys. Rev. D* **70** (2004) 012007, arXiv:[hep-ex/0403002](#) [hep-ex].
- [3] Belle Collaboration, T. Higuchi et al., *Search for Time-Dependent CPT Violation in Hadronic and Semileptonic B Decays*, *Phys. Rev. D* **85** (2012) 071105, arXiv:[1203.0930](#) [hep-ex].
- [4] LHCb Collaboration, R. Aaij et al., *Measurements of the B^+ , B^0 , B_s^0 meson and Λ_b^0 baryon lifetimes*, *JHEP* **04** (2014) 114, arXiv:[1402.2554](#) [hep-ex].
- [5] K. A. Olive et al., *Review of Particle Physics*, *Chin. Phys. C* **38** (2014) 090001.
- [6] C. Bobeth et al., *On new physics in $\Delta\Gamma_d$* , *JHEP* **06** (2014) 040, arXiv:[1404.2531](#) [hep-ph].
- [7] T. Gershon, $\Delta\Gamma_d$: A Forgotten Null Test of the Standard Model, *J. Phys. G* **38** (2011) 015007, arXiv:[1007.5135](#) [hep-ph].
- [8] I. Dunietz, R. Fleischer and U. Nierste, *In pursuit of new physics with B_s decays*, *Phys. Rev. D* **63** (2001) 114015, arXiv:[hep-ph/0012219](#) [hep-ph].
- [9] Y. Amhis et al., *Averages of b-hadron, c-hadron, and τ -lepton properties as of summer 2014*, (2014), arXiv:[1412.7515](#) [hep-ex].
- [10] E. Norrbin and R. Vogt, ‘Bottom production asymmetries at the LHC’, *Fifth Workshop on electronics for LHC experiments, Snowmass, CO, USA, 20-24 Sep 1999: Proceedings*, 2000, arXiv:[hep-ph/0003056](#) [hep-ph].
- [11] E. Norrbin and T. Sjöstrand, *Production and hadronization of heavy quarks*, *Eur. Phys. J. C* **17** (2000) 137–161, arXiv:[hep-ph/0005110](#) [hep-ph].
- [12] LHCb Collaboration, R. Aaij et al., *Measurement of the $\bar{B}^0 - B^0$ and $\bar{B}_s^0 - B_s^0$ production asymmetries in pp collisions at $\sqrt{s} = 7$ TeV*, *Phys. Lett. B* **739** (2014) 218–228, arXiv:[1408.0275](#) [hep-ex].
- [13] ATLAS Collaboration, *The ATLAS Experiment at the CERN Large Hadron Collider*, *JINST* **3** (2008) S08003.
- [14] ATLAS Collaboration, *Performance of the ATLAS Trigger System in 2010*, *Eur. Phys. J. C* **72** (2012) 1849, arXiv:[1110.1530](#) [hep-ex].
- [15] ATLAS Collaboration, *Performance of the ATLAS muon trigger in pp collisions at $\sqrt{s} = 8$ TeV*, *Eur. Phys. J. C* **75** (2015) 120, arXiv:[1408.3179](#) [hep-ex].
- [16] T. Sjöstrand, S. Mrenna and P. Z. Skands, *PYTHIA 6.4 Physics and Manual*, *JHEP* **05** (2006) 026, arXiv:[hep-ph/0603175](#) [hep-ph].
- [17] T. Sjöstrand, S. Mrenna and P. Z. Skands, *A Brief Introduction to PYTHIA 8.1*, *Comput. Phys. Commun.* **178** (2008) 852–867, arXiv:[0710.3820](#) [hep-ph].
- [18] ATLAS Collaboration, ‘ATLAS tunes of PYTHIA 6 and Pythia 8 for MC11’, tech. rep. ATL-PHYS-PUB-2011-009, CERN, July 2011, URL: <http://cdsweb.cern.ch/record/1363300>.
- [19] ATLAS Collaboration, *The ATLAS Simulation Infrastructure*, *Eur. Phys. J. C* **70** (2010) 823, arXiv:[1005.4568](#) [hep-ex].
- [20] S. Agostinelli et al., *GEANT4: A Simulation toolkit*, *Nucl. Instrum. Meth. A* **506** (2003) 250–303.

- [21] J. Allison et al., *Geant4 developments and applications*, *IEEE Trans. Nucl. Sci.* **53** (2006) 270.
- [22] LHCb Collaboration, R. Aaij et al., *Measurement of the effective $B_s^0 \rightarrow J/\psi K_S^0$ lifetime*, *Nucl. Phys. B* **873** (2013) 275–292, arXiv:1304.4500 [hep-ex].
- [23] D0 Collaboration, V. Abazov et al.,
Study of CP-violating charge asymmetries of single muons and like-sign dimuons in $p\bar{p}$ collisions, *Phys. Rev. D* **89** (2014) 012002, arXiv:1310.0447 [hep-ex].

The ATLAS Collaboration

M. Aaboud^{136d}, G. Aad⁸⁷, B. Abbott¹¹⁴, J. Abdallah⁶⁵, O. Abdinov¹², B. Abelsoos¹¹⁸, R. Aben¹⁰⁸, O.S. AbouZeid¹³⁸, N.L. Abraham¹⁵⁰, H. Abramowicz¹⁵⁴, H. Abreu¹⁵³, R. Abreu¹¹⁷, Y. Abulaiti^{147a,147b}, B.S. Acharya^{164a,164b,a}, L. Adamczyk^{40a}, D.L. Adams²⁷, J. Adelman¹⁰⁹, S. Adomeit¹⁰¹, T. Adye¹³², A.A. Affolder⁷⁶, T. Agatonovic-Jovin¹⁴, J. Agricola⁵⁶, J.A. Aguilar-Saavedra^{127a,127f}, S.P. Ahlen²⁴, F. Ahmadov^{67,b}, G. Aielli^{134a,134b}, H. Akerstedt^{147a,147b}, T.P.A. Åkesson⁸³, A.V. Akimov⁹⁷, G.L. Alberghi^{22a,22b}, J. Albert¹⁶⁹, S. Albrand⁵⁷, M.J. Alconada Verzini⁷³, M. Alekса³², I.N. Aleksandrov⁶⁷, C. Alexa^{28b}, G. Alexander¹⁵⁴, T. Alexopoulos¹⁰, M. Alhroob¹¹⁴, M. Aliev^{75a,75b}, G. Alimonti^{93a}, J. Alison³³, S.P. Alkire³⁷, B.M.M. Allbrooke¹⁵⁰, B.W. Allen¹¹⁷, P.P. Allport¹⁹, A. Aloisio^{105a,105b}, A. Alonso³⁸, F. Alonso⁷³, C. Alpigiani¹³⁹, M. Alstaty⁸⁷, B. Alvarez Gonzalez³², D. Álvarez Piqueras¹⁶⁷, M.G. Alviggi^{105a,105b}, B.T. Amadio¹⁶, K. Amako⁶⁸, Y. Amaral Coutinho^{26a}, C. Amelung²⁵, D. Amidei⁹¹, S.P. Amor Dos Santos^{127a,127c}, A. Amorim^{127a,127b}, S. Amoroso³², G. Amundsen²⁵, C. Anastopoulos¹⁴⁰, L.S. Ansu⁵¹, N. Andari¹⁰⁹, T. Andeen¹¹, C.F. Anders^{60b}, G. Anders³², J.K. Anders⁷⁶, K.J. Anderson³³, A. Andreazza^{93a,93b}, V. Andrei^{60a}, S. Angelidakis⁹, I. Angelozzi¹⁰⁸, P. Anger⁴⁶, A. Angerami³⁷, F. Anghinolfi³², A.V. Anisenkov^{110,c}, N. Anjos¹³, A. Annovi^{125a,125b}, M. Antonelli⁴⁹, A. Antonov⁹⁹, F. Anulli^{133a}, M. Aoki⁶⁸, L. Aperio Bella¹⁹, G. Arabidze⁹², Y. Arai⁶⁸, J.P. Araque^{127a}, A.T.H. Arce⁴⁷, F.A. Arduh⁷³, J.-F. Arguin⁹⁶, S. Argyropoulos⁶⁵, M. Arik^{20a}, A.J. Armbruster¹⁴⁴, L.J. Armitage⁷⁸, O. Arnaez³², H. Arnold⁵⁰, M. Arratia³⁰, O. Arslan²³, A. Artamonov⁹⁸, G. Artoni¹²¹, S. Artz⁸⁵, S. Asai¹⁵⁶, N. Asbah⁴⁴, A. Ashkenazi¹⁵⁴, B. Åsman^{147a,147b}, L. Asquith¹⁵⁰, K. Assamagan²⁷, R. Astalos^{145a}, M. Atkinson¹⁶⁶, N.B. Atlay¹⁴², K. Augsten¹²⁹, G. Avolio³², B. Axen¹⁶, M.K. Ayoub¹¹⁸, G. Azuelos^{96,d}, M.A. Baak³², A.E. Baas^{60a}, M.J. Baca¹⁹, H. Bachacou¹³⁷, K. Bachas^{75a,75b}, M. Backes³², M. Backhaus³², P. Bagiacchi^{133a,133b}, P. Bagnaia^{133a,133b}, Y. Bai^{35a}, J.T. Barnes¹³², O.K. Baker¹⁷⁶, E.M. Baldin^{110,c}, P. Balek¹³⁰, T. Balestri¹⁴⁹, F. Balli¹³⁷, W.K. Balunas¹²³, E. Banas⁴¹, Sw. Banerjee^{173,e}, A.A.E. Bannoura¹⁷⁵, L. Barak³², E.L. Barberio⁹⁰, D. Barberis^{52a,52b}, M. Barbero⁸⁷, T. Barillari¹⁰², T. Barklow¹⁴⁴, N. Barlow³⁰, S.L. Barnes⁸⁶, B.M. Barnett¹³², R.M. Barnett¹⁶, Z. Barnovska⁵, A. Baroncelli^{135a}, G. Barone²⁵, A.J. Barr¹²¹, L. Barranco Navarro¹⁶⁷, F. Barreiro⁸⁴, J. Barreiro Guimarães da Costa^{35a}, R. Bartoldus¹⁴⁴, A.E. Barton⁷⁴, P. Bartos^{145a}, A. Basalaev¹²⁴, A. Bassalat¹¹⁸, R.L. Bates⁵⁵, S.J. Batista¹⁵⁹, J.R. Batley³⁰, M. Battaglia¹³⁸, M. Bauce^{133a,133b}, F. Bauer¹³⁷, H.S. Bawa^{144,f}, J.B. Beacham¹¹², M.D. Beattie⁷⁴, T. Beau⁸², P.H. Beauchemin¹⁶², P. Bechtle²³, H.P. Beck^{18,g}, K. Becker¹²¹, M. Becker⁸⁵, M. Beckingham¹⁷⁰, C. Becot¹¹¹, A.J. Beddall^{20e}, A. Beddall^{20b}, V.A. Bednyakov⁶⁷, M. Bedognetti¹⁰⁸, C.P. Bee¹⁴⁹, L.J. Beemster¹⁰⁸, T.A. Beermann³², M. Begel²⁷, J.K. Behr⁴⁴, C. Belanger-Champagne⁸⁹, A.S. Bell⁸⁰, G. Bella¹⁵⁴, L. Bellagamba^{22a}, A. Bellerive³¹, M. Bellomo⁸⁸, K. Belotskiy⁹⁹, O. Beltramello³², N.L. Belyaev⁹⁹, O. Benary¹⁵⁴, D. Benchekroun^{136a}, M. Bender¹⁰¹, K. Bendtz^{147a,147b}, N. Benekos¹⁰, Y. Benhammou¹⁵⁴, E. Benhar Noccioli¹⁷⁶, J. Benitez⁶⁵, D.P. Benjamin⁴⁷, J.R. Bensinger²⁵, S. Bentvelsen¹⁰⁸, L. Beresford¹²¹, M. Beretta⁴⁹, D. Berge¹⁰⁸, E. Bergeaas Kuutmann¹⁶⁵, N. Berger⁵, J. Beringer¹⁶, S. Berlendis⁵⁷, N.R. Bernard⁸⁸, C. Bernius¹¹¹, F.U. Bernlochner²³, T. Berry⁷⁹, P. Berta¹³⁰, C. Bertella⁸⁵, G. Bertoli^{147a,147b}, F. Bertolucci^{125a,125b}, I.A. Bertram⁷⁴, C. Bertsche⁴⁴, D. Bertsche¹¹⁴, G.J. Besjes³⁸, O. Bessidskaia Bylund^{147a,147b}, M. Bessner⁴⁴, N. Besson¹³⁷, C. Betancourt⁵⁰, S. Bethke¹⁰², A.J. Bevan⁷⁸, W. Bhimji¹⁶, R.M. Bianchi¹²⁶, L. Bianchini²⁵, M. Bianco³², O. Biebel¹⁰¹, D. Biedermann¹⁷, R. Bielski⁸⁶, N.V. Biesuz^{125a,125b}, M. Biglietti^{135a}, J. Bilbao De Mendizabal⁵¹, H. Bilonok⁴⁹, M. Bindi⁵⁶, S. Binet¹¹⁸, A. Bingul^{20b}, C. Bini^{133a,133b}, S. Biondi^{22a,22b}, D.M. Bjergaard⁴⁷, C.W. Black¹⁵¹, J.E. Black¹⁴⁴, K.M. Black²⁴, D. Blackburn¹³⁹, R.E. Blair⁶, J.-B. Blanchard¹³⁷, J.E. Blanco⁷⁹, T. Blazek^{145a}, I. Bloch⁴⁴, C. Blocker²⁵, W. Blum^{85,*}, U. Blumenschein⁵⁶, S. Blunier^{34a},

G.J. Bobbink¹⁰⁸, V.S. Bobrovnikov^{110,c}, S.S. Bocchetta⁸³, A. Bocci⁴⁷, C. Bock¹⁰¹, M. Boehler⁵⁰,
 D. Boerner¹⁷⁵, J.A. Bogaerts³², D. Bogavac¹⁴, A.G. Bogdanchikov¹¹⁰, C. Bohm^{147a}, V. Boisvert⁷⁹,
 P. Bokan¹⁴, T. Bold^{40a}, A.S. Boldyrev^{164a,164c}, M. Bomben⁸², M. Bona⁷⁸, M. Boonekamp¹³⁷,
 A. Borisov¹³¹, G. Borissov⁷⁴, J. Bortfeldt¹⁰¹, D. Bortoletto¹²¹, V. Bortolotto^{62a,62b,62c}, K. Bos¹⁰⁸,
 D. Boscherini^{22a}, M. Bosman¹³, J.D. Bossio Sola²⁹, J. Boudreau¹²⁶, J. Bouffard²,
 E.V. Bouhova-Thacker⁷⁴, D. Boumediene³⁶, C. Bourdarios¹¹⁸, S.K. Boutle⁵⁵, A. Boveia³², J. Boyd³²,
 I.R. Boyko⁶⁷, J. Bracinik¹⁹, A. Brandt⁸, G. Brandt⁵⁶, O. Brandt^{60a}, U. Bratzler¹⁵⁷, B. Brau⁸⁸,
 J.E. Brau¹¹⁷, H.M. Braun^{175,*}, W.D. Breaden Madden⁵⁵, K. Brendlinger¹²³, A.J. Brennan⁹⁰,
 L. Brenner¹⁰⁸, R. Brenner¹⁶⁵, S. Bressler¹⁷², T.M. Bristow⁴⁸, D. Britton⁵⁵, D. Britzger⁴⁴, F.M. Brochu³⁰,
 I. Brock²³, R. Brock⁹², G. Brooijmans³⁷, T. Brooks⁷⁹, W.K. Brooks^{34b}, J. Brosamer¹⁶, E. Brost¹¹⁷,
 J.H. Broughton¹⁹, P.A. Bruckman de Renstrom⁴¹, D. Bruncko^{145b}, R. Bruneliere⁵⁰, A. Bruni^{22a},
 G. Bruni^{22a}, L.S. Bruni¹⁰⁸, BH Brunt³⁰, M. Bruschi^{22a}, N. Bruscino²³, P. Bryant³³, L. Bryngemark⁸³,
 T. Buanes¹⁵, Q. Buat¹⁴³, P. Buchholz¹⁴², A.G. Buckley⁵⁵, I.A. Budagov⁶⁷, F. Buehrer⁵⁰, M.K. Bugge¹²⁰,
 O. Bulekov⁹⁹, D. Bullock⁸, H. Burckhart³², S. Burdin⁷⁶, C.D. Burgard⁵⁰, B. Burghgrave¹⁰⁹, K. Burka⁴¹,
 S. Burke¹³², I. Burmeister⁴⁵, E. Busato³⁶, D. Büscher⁵⁰, V. Büscher⁸⁵, P. Bussey⁵⁵, J.M. Butler²⁴,
 C.M. Buttar⁵⁵, J.M. Butterworth⁸⁰, P. Butti¹⁰⁸, W. Buttlinger²⁷, A. Buzatu⁵⁵, A.R. Buzykaev^{110,c},
 S. Cabrera Urbán¹⁶⁷, D. Caforio¹²⁹, V.M. Cairo^{39a,39b}, O. Cakir^{4a}, N. Calace⁵¹, P. Calafuria¹⁶,
 A. Calandri⁸⁷, G. Calderini⁸², P. Calfayan¹⁰¹, L.P. Caloba^{26a}, D. Calvet³⁶, S. Calvet³⁶, T.P. Calvet⁸⁷,
 R. Camacho Toro³³, S. Camarda³², P. Camarri^{134a,134b}, D. Cameron¹²⁰, R. Caminal Armadans¹⁶⁶,
 C. Camincher⁵⁷, S. Campana³², M. Campanelli⁸⁰, A. Camplani^{93a,93b}, A. Campoverde¹⁴²,
 V. Canale^{105a,105b}, A. Canepa^{160a}, M. Cano Bret^{35e}, J. Cantero¹¹⁵, R. Cantrill^{127a}, T. Cao⁴²,
 M.D.M. Capeans Garrido³², I. Caprini^{28b}, M. Caprini^{28b}, M. Capua^{39a,39b}, R. Caputo⁸⁵, R.M. Carbone³⁷,
 R. Cardarelli^{134a}, F. Cardillo⁵⁰, I. Carli¹³⁰, T. Carli³², G. Carlino^{105a}, L. Carminati^{93a,93b}, S. Caron¹⁰⁷,
 E. Carquin^{34b}, G.D. Carrillo-Montoya³², J.R. Carter³⁰, J. Carvalho^{127a,127c}, D. Casadei¹⁹,
 M.P. Casado^{13,h}, M. Casolino¹³, D.W. Casper¹⁶³, E. Castaneda-Miranda^{146a}, R. Castelijn¹⁰⁸,
 A. Castelli¹⁰⁸, V. Castillo Gimenez¹⁶⁷, N.F. Castro^{127a,i}, A. Catinaccio³², J.R. Catmore¹²⁰, A. Cattai³²,
 J. Caudron⁸⁵, V. Cavalieri¹⁶⁶, E. Cavallaro¹³, D. Cavalli^{93a}, M. Cavalli-Sforza¹³, V. Cavasinni^{125a,125b},
 F. Ceradini^{135a,135b}, L. Cerdá Alberich¹⁶⁷, B.C. Cerio⁴⁷, A.S. Cerqueira^{26b}, A. Cerri¹⁵⁰, L. Cerrito⁷⁸,
 F. Cerutti¹⁶, M. Cerv³², A. Cervelli¹⁸, S.A. Cetin^{20d}, A. Chafaq^{136a}, D. Chakraborty¹⁰⁹, S.K. Chan⁵⁹,
 Y.L. Chan^{62a}, P. Chang¹⁶⁶, J.D. Chapman³⁰, D.G. Charlton¹⁹, A. Chatterjee⁵¹, C.C. Chau¹⁵⁹,
 C.A. Chavez Barajas¹⁵⁰, S. Che¹¹², S. Cheatham⁷⁴, A. Chegwidden⁹², S. Chekanov⁶,
 S.V. Chekulaev^{160a}, G.A. Chelkov^{67,j}, M.A. Chelstowska⁹¹, C. Chen⁶⁶, H. Chen²⁷, K. Chen¹⁴⁹,
 S. Chen^{35c}, S. Chen¹⁵⁶, X. Chen^{35f}, Y. Chen⁶⁹, H.C. Cheng⁹¹, H.J. Cheng^{35a}, Y. Cheng³³,
 A. Cheplakov⁶⁷, E. Cheremushkina¹³¹, R. Cherkaoui El Moursli^{136e}, V. Chernyatin^{27,*}, E. Cheu⁷,
 L. Chevalier¹³⁷, V. Chiarella⁴⁹, G. Chiarelli^{125a,125b}, G. Chiodini^{75a}, A.S. Chisholm¹⁹, A. Chitan^{28b},
 M.V. Chizhov⁶⁷, K. Choi⁶³, A.R. Chomont³⁶, S. Chouridou⁹, B.K.B. Chow¹⁰¹, V. Christodoulou⁸⁰,
 D. Chromek-Burckhardt³², J. Chudoba¹²⁸, A.J. Chuinard⁸⁹, J.J. Chwastowski⁴¹, L. Chytka¹¹⁶,
 G. Ciapetti^{133a,133b}, A.K. Ciftci^{4a}, D. Cinca⁵⁵, V. Cindro⁷⁷, I.A. Cioara²³, A. Ciocio¹⁶, F. Cirotto^{105a,105b},
 Z.H. Citron¹⁷², M. Citterio^{93a}, M. Ciubancan^{28b}, A. Clark⁵¹, B.L. Clark⁵⁹, M.R. Clark³⁷, P.J. Clark⁴⁸,
 R.N. Clarke¹⁶, C. Clement^{147a,147b}, Y. Coadou⁸⁷, M. Cobal^{164a,164c}, A. Coccaro⁵¹, J. Cochran⁶⁶,
 L. Coffey²⁵, L. Colasurdo¹⁰⁷, B. Cole³⁷, A.P. Colijn¹⁰⁸, J. Collot⁵⁷, T. Colombo³², G. Compostella¹⁰²,
 P. Conde Muiño^{127a,127b}, E. Coniavitis⁵⁰, S.H. Connell^{146b}, I.A. Connolly⁷⁹, V. Consorti⁵⁰,
 S. Constantinescu^{28b}, G. Conti³², F. Conventi^{105a,k}, M. Cooke¹⁶, B.D. Cooper⁸⁰, A.M. Cooper-Sarkar¹²¹,
 K.J.R. Cormier¹⁵⁹, T. Cornelissen¹⁷⁵, M. Corradi^{133a,133b}, F. Corriveau^{89,l}, A. Corso-Radu¹⁶³,
 A. Cortes-Gonzalez¹³, G. Cortiana¹⁰², G. Costa^{93a}, M.J. Costa¹⁶⁷, D. Costanzo¹⁴⁰, G. Cottin³⁰,
 G. Cowan⁷⁹, B.E. Cox⁸⁶, K. Cranmer¹¹¹, S.J. Crawley⁵⁵, G. Cree³¹, S. Crépé-Renaudin⁵⁷, F. Crescioli⁸²,
 W.A. Cribbs^{147a,147b}, M. Crispin Ortuzar¹²¹, M. Cristinziani²³, V. Croft¹⁰⁷, G. Crosetti^{39a,39b},

T. Cuhadar Donszelmann¹⁴⁰, J. Cummings¹⁷⁶, M. Curatolo⁴⁹, J. Cúth⁸⁵, C. Cuthbert¹⁵¹, H. Czirr¹⁴²,
 P. Czodrowski³, G. D'amen^{22a,22b}, S. D'Auria⁵⁵, M. D'Onofrio⁷⁶,
 M.J. Da Cunha Sargedas De Sousa^{127a,127b}, C. Da Via⁸⁶, W. Dabrowski^{40a}, T. Dado^{145a}, T. Dai⁹¹,
 O. Dale¹⁵, F. Dallaire⁹⁶, C. Dallapiccola⁸⁸, M. Dam³⁸, J.R. Dandoy³³, N.P. Dang⁵⁰, A.C. Daniells¹⁹,
 N.S. Dann⁸⁶, M. Danninger¹⁶⁸, M. Dano Hoffmann¹³⁷, V. Dao⁵⁰, G. Darbo^{52a}, S. Darmora⁸,
 J. Dassoulas³, A. Dattagupta⁶³, W. Davey²³, C. David¹⁶⁹, T. Davidek¹³⁰, M. Davies¹⁵⁴, P. Davison⁸⁰,
 E. Dawe⁹⁰, I. Dawson¹⁴⁰, R.K. Daya-Ishmukhametova⁸⁸, K. De⁸, R. de Asmundis^{105a},
 A. De Benedetti¹¹⁴, S. De Castro^{22a,22b}, S. De Cecco⁸², N. De Groot¹⁰⁷, P. de Jong¹⁰⁸, H. De la Torre⁸⁴,
 F. De Lorenzi⁶⁶, A. De Maria⁵⁶, D. De Pedis^{133a}, A. De Salvo^{133a}, U. De Sanctis¹⁵⁰, A. De Santo¹⁵⁰,
 J.B. De Vivie De Regie¹¹⁸, W.J. Dearnaley⁷⁴, R. Debbe²⁷, C. Debenedetti¹³⁸, D.V. Dedovich⁶⁷,
 N. Dehghanian³, I. Deigaard¹⁰⁸, M. Del Gaudio^{39a,39b}, J. Del Peso⁸⁴, T. Del Prete^{125a,125b},
 D. Delgove¹¹⁸, F. Deliot¹³⁷, C.M. Delitzsch⁵¹, M. Deliyergiyev⁷⁷, A. Dell'Acqua³², L. Dell'Asta²⁴,
 M. Dell'Orso^{125a,125b}, M. Della Pietra^{105a,k}, D. della Volpe⁵¹, M. Delmastro⁵, P.A. Delsart⁵⁷,
 C. Deluca¹⁰⁸, D.A. DeMarco¹⁵⁹, S. Demers¹⁷⁶, M. Demichev⁶⁷, A. Demilly⁸², S.P. Denisov¹³¹,
 D. Denysiuk¹³⁷, D. Derendarz⁴¹, J.E. Derkaoui^{136d}, F. Derue⁸², P. Dervan⁷⁶, K. Desch²³, C. Deterre⁴⁴,
 K. Dette⁴⁵, P.O. Deviveiros³², A. Dewhurst¹³², S. Dhaliwal²⁵, A. Di Ciacio^{134a,134b}, L. Di Ciacio⁵,
 W.K. Di Clemente¹²³, C. Di Donato^{133a,133b}, A. Di Girolamo³², B. Di Girolamo³², B. Di Micco^{135a,135b},
 R. Di Nardo³², A. Di Simone⁵⁰, R. Di Sipio¹⁵⁹, D. Di Valentino³¹, C. Diaconu⁸⁷, M. Diamond¹⁵⁹,
 F.A. Dias⁴⁸, M.A. Diaz^{34a}, E.B. Diehl⁹¹, J. Dietrich¹⁷, S. Diglio⁸⁷, A. Dimitrieva¹⁴, J. Dingfelder²³,
 P. Dita^{28b}, S. Dita^{28b}, F. Dittus³², F. Djama⁸⁷, T. Djobava^{53b}, J.I. Djuvsland^{60a}, M.A.B. do Vale^{26c},
 D. Dobos³², M. Dobre^{28b}, C. Doglioni⁸³, T. Dohmae¹⁵⁶, J. Dolejsi¹³⁰, Z. Dolezal¹³⁰,
 B.A. Dolgoshein^{99,*}, M. Donadelli^{26d}, S. Donati^{125a,125b}, P. Dondero^{122a,122b}, J. Donini³⁶, J. Dopke¹³²,
 A. Doria^{105a}, M.T. Dova⁷³, A.T. Doyle⁵⁵, E. Drechsler⁵⁶, M. Dris¹⁰, Y. Du^{35d}, J. Duarte-Campderros¹⁵⁴,
 E. Duchovni¹⁷², G. Duckeck¹⁰¹, O.A. Ducu^{96,m}, D. Duda¹⁰⁸, A. Dudarev³², E.M. Duffield¹⁶,
 L. Duflot¹¹⁸, L. Duguid⁷⁹, M. Dührssen³², M. Dumancic¹⁷², M. Dunford^{60a}, H. Duran Yildiz^{4a},
 M. Düren⁵⁴, A. Durglishvili^{53b}, D. Duschinger⁴⁶, B. Dutta⁴⁴, M. Dyndal⁴⁴, C. Eckardt⁴⁴, K.M. Ecker¹⁰²,
 R.C. Edgar⁹¹, N.C. Edwards⁴⁸, T. Eifert³², G. Eigen¹⁵, K. Einsweiler¹⁶, T. Ekelof¹⁶⁵, M. El Kacimi^{136c},
 V. Ellajosyula⁸⁷, M. Ellert¹⁶⁵, S. Elles⁵, F. Ellinghaus¹⁷⁵, A.A. Elliott¹⁶⁹, N. Ellis³², J. Elmsheuser²⁷,
 M. Elsing³², D. Emeliyanov¹³², Y. Enari¹⁵⁶, O.C. Endner⁸⁵, M. Endo¹¹⁹, J.S. Ennis¹⁷⁰, J. Erdmann⁴⁵,
 A. Ereditato¹⁸, G. Ernis¹⁷⁵, J. Ernst², M. Ernst²⁷, S. Errede¹⁶⁶, E. Ertel⁸⁵, M. Escalier¹¹⁸, H. Esch⁴⁵,
 C. Escobar¹²⁶, B. Esposito⁴⁹, A.I. Etienvre¹³⁷, E. Etzion¹⁵⁴, H. Evans⁶³, A. Ezhilov¹²⁴, F. Fabbri^{22a,22b},
 L. Fabbri^{22a,22b}, G. Facini³³, R.M. Fakhrutdinov¹³¹, S. Falciano^{133a}, R.J. Falla⁸⁰, J. Faltova¹³⁰,
 Y. Fang^{35a}, M. Fanti^{93a,93b}, A. Farbin⁸, A. Farilla^{135a}, C. Farina¹²⁶, T. Farooque¹³, S. Farrell¹⁶,
 S.M. Farrington¹⁷⁰, P. Farthouat³², F. Fassi^{136e}, P. Fassnacht³², D. Fassouliotis⁹, M. Fucci Giannelli⁷⁹,
 A. Favareto^{52a,52b}, W.J. Fawcett¹²¹, L. Fayard¹¹⁸, O.L. Fedin^{124,n}, W. Fedorko¹⁶⁸, S. Feigl¹²⁰,
 L. Feligioni⁸⁷, C. Feng^{35d}, E.J. Feng³², H. Feng⁹¹, A.B. Fenyuk¹³¹, L. Feremenga⁸,
 P. Fernandez Martinez¹⁶⁷, S. Fernandez Perez¹³, J. Ferrando⁵⁵, A. Ferrari¹⁶⁵, P. Ferrari¹⁰⁸, R. Ferrari^{122a},
 D.E. Ferreira de Lima^{60b}, A. Ferrer¹⁶⁷, D. Ferrere⁵¹, C. Ferretti⁹¹, A. Ferretto Parodi^{52a,52b}, F. Fiedler⁸⁵,
 A. Filipčič⁷⁷, M. Filipuzzi⁴⁴, F. Filthaut¹⁰⁷, M. Fincke-Keeler¹⁶⁹, K.D. Finelli¹⁵¹,
 M.C.N. Fiolhais^{127a,127c}, L. Fiorini¹⁶⁷, A. Firan⁴², A. Fischer², C. Fischer¹³, J. Fischer¹⁷⁵, W.C. Fisher⁹²,
 N. Flaschel⁴⁴, I. Fleck¹⁴², P. Fleischmann⁹¹, G.T. Fletcher¹⁴⁰, R.R.M. Fletcher¹²³, T. Flick¹⁷⁵,
 A. Floderus⁸³, L.R. Flores Castillo^{62a}, M.J. Flowerdew¹⁰², G.T. Forcolin⁸⁶, A. Formica¹³⁷, A. Forti⁸⁶,
 A.G. Foster¹⁹, D. Fournier¹¹⁸, H. Fox⁷⁴, S. Fracchia¹³, P. Francavilla⁸², M. Franchini^{22a,22b},
 D. Francis³², L. Franconi¹²⁰, M. Franklin⁵⁹, M. Frate¹⁶³, M. Fraternali^{122a,122b}, D. Freeborn⁸⁰,
 S.M. Fressard-Batraneanu³², F. Friedrich⁴⁶, D. Froidevaux³², J.A. Frost¹²¹, C. Fukunaga¹⁵⁷,
 E. Fullana Torregrossa⁸⁵, T. Fusayasu¹⁰³, J. Fuster¹⁶⁷, C. Gabaldon⁵⁷, O. Gabizon¹⁷⁵, A. Gabrielli^{22a,22b},
 A. Gabrielli¹⁶, G.P. Gach^{40a}, S. Gadatsch³², S. Gadomski⁵¹, G. Gagliardi^{52a,52b}, L.G. Gagnon⁹⁶,

P. Gagnon⁶³, C. Galea¹⁰⁷, B. Galhardo^{127a,127c}, E.J. Gallas¹²¹, B.J. Gallop¹³², P. Gallus¹²⁹, G. Galster³⁸, K.K. Gan¹¹², J. Gao^{35b,87}, Y. Gao⁴⁸, Y.S. Gao^{144,f}, F.M. Garay Walls⁴⁸, C. García¹⁶⁷, J.E. García Navarro¹⁶⁷, M. Garcia-Sciveres¹⁶, R.W. Gardner³³, N. Garelli¹⁴⁴, V. Garonne¹²⁰, A. Gascon Bravo⁴⁴, C. Gatti⁴⁹, A. Gaudiello^{52a,52b}, G. Gaudio^{122a}, B. Gaur¹⁴², L. Gauthier⁹⁶, I.L. Gavrilenko⁹⁷, C. Gay¹⁶⁸, G. Gaycken²³, E.N. Gazis¹⁰, Z. Gecse¹⁶⁸, C.N.P. Gee¹³², Ch. Geich-Gimbel²³, M. Geisen⁸⁵, M.P. Geisler^{60a}, C. Gemme^{52a}, M.H. Genest⁵⁷, C. Geng^{35b,o}, S. Gentile^{133a,133b}, S. George⁷⁹, D. Gerbaudo¹³, A. Gershon¹⁵⁴, S. Ghasemi¹⁴², H. Ghazlane^{136b}, M. Ghneimat²³, B. Giacobbe^{22a}, S. Giagu^{133a,133b}, P. Giannetti^{125a,125b}, B. Gibbard²⁷, S.M. Gibson⁷⁹, M. Gignac¹⁶⁸, M. Gilchriese¹⁶, T.P.S. Gillam³⁰, D. Gillberg³¹, G. Gilles¹⁷⁵, D.M. Gingrich^{3,d}, N. Giokaris⁹, M.P. Giordani^{164a,164c}, F.M. Giorgi^{22a}, F.M. Giorgi¹⁷, P.F. Giraud¹³⁷, P. Giromini⁵⁹, D. Giugni^{93a}, F. Giuli¹²¹, C. Giuliani¹⁰², M. Giulini^{60b}, B.K. Gjelsten¹²⁰, S. Gkaitatzis¹⁵⁵, I. Gkialas¹⁵⁵, E.L. Gkougkousis¹¹⁸, L.K. Gladilin¹⁰⁰, C. Glasman⁸⁴, J. Glatzer³², P.C.F. Glaysher⁴⁸, A. Glazov⁴⁴, M. Goblirsch-Kolb¹⁰², J. Godlewski⁴¹, S. Goldfarb⁹¹, T. Golling⁵¹, D. Golubkov¹³¹, A. Gomes^{127a,127b,127d}, R. Gonçalo^{127a}, J. Goncalves Pinto Firmino Da Costa¹³⁷, G. Gonella⁵⁰, L. Gonella¹⁹, A. Gongadze⁶⁷, S. González de la Hoz¹⁶⁷, G. Gonzalez Parra¹³, S. Gonzalez-Sevilla⁵¹, L. Goossens³², P.A. Gorbounov⁹⁸, H.A. Gordon²⁷, I. Gorelov¹⁰⁶, B. Gorini³², E. Gorini^{75a,75b}, A. Gorišek⁷⁷, E. Gornicki⁴¹, A.T. Goshaw⁴⁷, C. Gössling⁴⁵, M.I. Gostkin⁶⁷, C.R. Goudet¹¹⁸, D. Goujdami^{136c}, A.G. Goussiou¹³⁹, N. Govender^{146b,p}, E. Gozani¹⁵³, L. Graber⁵⁶, I. Grabowska-Bold^{40a}, P.O.J. Gradin⁵⁷, P. Grafström^{22a,22b}, J. Gramling⁵¹, E. Gramstad¹²⁰, S. Grancagnolo¹⁷, V. Gratchev¹²⁴, P.M. Gravila^{28e}, H.M. Gray³², E. Graziani^{135a}, Z.D. Greenwood^{81,q}, C. Grefe²³, K. Gregersen⁸⁰, I.M. Gregor⁴⁴, P. Grenier¹⁴⁴, K. Grevtsov⁵, J. Griffiths⁸, A.A. Grillo¹³⁸, K. Grimm⁷⁴, S. Grinstein^{13,r}, Ph. Gris³⁶, J.-F. Grivaz¹¹⁸, S. Groh⁸⁵, J.P. Grohs⁴⁶, E. Gross¹⁷², J. Grosse-Knetter⁵⁶, G.C. Grossi⁸¹, Z.J. Grout¹⁵⁰, L. Guan⁹¹, W. Guan¹⁷³, J. Guenther¹²⁹, F. Guescini⁵¹, D. Guest¹⁶³, O. Gueta¹⁵⁴, E. Guido^{52a,52b}, T. Guillemin⁵, S. Guindon², U. Gul⁵⁵, C. Gumpert³², J. Guo^{35e}, Y. Guo^{35b,o}, S. Gupta¹²¹, G. Gustavino^{133a,133b}, P. Gutierrez¹¹⁴, N.G. Gutierrez Ortiz⁸⁰, C. Gutschow⁴⁶, C. Guyot¹³⁷, C. Gwenlan¹²¹, C.B. Gwilliam⁷⁶, A. Haas¹¹¹, C. Haber¹⁶, H.K. Hadavand⁸, N. Haddad^{136e}, A. Hadef⁸⁷, P. Haefner²³, S. Hageböck²³, Z. Hajduk⁴¹, H. Hakobyan^{177,*}, M. Haleem⁴⁴, J. Haley¹¹⁵, G. Halladjian⁹², G.D. Hallewell⁸⁷, K. Hamacher¹⁷⁵, P. Hamal¹¹⁶, K. Hamano¹⁶⁹, A. Hamilton^{146a}, G.N. Hamity¹⁴⁰, P.G. Hamnett⁴⁴, L. Han^{35b}, K. Hanagaki^{68,s}, K. Hanawa¹⁵⁶, M. Hance¹³⁸, B. Haney¹²³, P. Hanke^{60a}, R. Hanna¹³⁷, J.B. Hansen³⁸, J.D. Hansen³⁸, M.C. Hansen²³, P.H. Hansen³⁸, K. Hara¹⁶¹, A.S. Hard¹⁷³, T. Harenberg¹⁷⁵, F. Hariri¹¹⁸, S. Harkusha⁹⁴, R.D. Harrington⁴⁸, P.F. Harrison¹⁷⁰, F. Hartjes¹⁰⁸, N.M. Hartmann¹⁰¹, M. Hasegawa⁶⁹, Y. Hasegawa¹⁴¹, A. Hasib¹¹⁴, S. Hassani¹³⁷, S. Haug¹⁸, R. Hauser⁹², L. Hauswald⁴⁶, M. Havranek¹²⁸, C.M. Hawkes¹⁹, R.J. Hawkings³², D. Hayden⁹², C.P. Hays¹²¹, J.M. Hays⁷⁸, H.S. Hayward⁷⁶, S.J. Haywood¹³², S.J. Head¹⁹, T. Heck⁸⁵, V. Hedberg⁸³, L. Heelan⁸, S. Heim¹²³, T. Heim¹⁶, B. Heinemann¹⁶, J.J. Heinrich¹⁰¹, L. Heinrich¹¹¹, C. Heinz⁵⁴, J. Hejbal¹²⁸, L. Helary²⁴, S. Hellman^{147a,147b}, C. Helsens³², J. Henderson¹²¹, R.C.W. Henderson⁷⁴, Y. Heng¹⁷³, S. Henkelmann¹⁶⁸, A.M. Henriques Correia³², S. Henrot-Versille¹¹⁸, G.H. Herbert¹⁷, Y. Hernández Jiménez¹⁶⁷, G. Herten⁵⁰, R. Hertenberger¹⁰¹, L. Hervas³², G.G. Hesketh⁸⁰, N.P. Hessey¹⁰⁸, J.W. Hetherly⁴², R. Hickling⁷⁸, E. Higón-Rodriguez¹⁶⁷, E. Hill¹⁶⁹, J.C. Hill³⁰, K.H. Hiller⁴⁴, S.J. Hillier¹⁹, I. Hinchliffe¹⁶, E. Hines¹²³, R.R. Hinman¹⁶, M. Hirose¹⁵⁸, D. Hirschbuehl¹⁷⁵, J. Hobbs¹⁴⁹, N. Hod^{160a}, M.C. Hodgkinson¹⁴⁰, P. Hodgson¹⁴⁰, A. Hoecker³², M.R. Hoeferkamp¹⁰⁶, F. Hoenig¹⁰¹, D. Hohn²³, T.R. Holmes¹⁶, M. Homann⁴⁵, T.M. Hong¹²⁶, B.H. Hooberman¹⁶⁶, W.H. Hopkins¹¹⁷, Y. Horii¹⁰⁴, A.J. Horton¹⁴³, J.-Y. Hostachy⁵⁷, S. Hou¹⁵², A. Hoummada^{136a}, J. Howarth⁴⁴, M. Hrabovsky¹¹⁶, I. Hristova¹⁷, J. Hrivnac¹¹⁸, T. Hrynevich⁹⁵, C. Hsu^{146c}, P.J. Hsu^{152,t}, S.-C. Hsu¹³⁹, D. Hu³⁷, Q. Hu^{35b}, Y. Huang⁴⁴, Z. Hubacek¹²⁹, F. Hubaut⁸⁷, F. Huegging²³, T.B. Huffman¹²¹, E.W. Hughes³⁷, G. Hughes⁷⁴, M. Huhtinen³², T.A. Hülsing⁸⁵, P. Huo¹⁴⁹, N. Huseynov^{67,b}, J. Huston⁹², J. Huth⁵⁹, G. Iacobucci⁵¹,

G. Iakovidis²⁷, I. Ibragimov¹⁴², L. Iconomidou-Fayard¹¹⁸, E. Ideal¹⁷⁶, Z. Idrissi^{136e}, P. Iengo³²,
 O. Igonkina^{108,u}, T. Iizawa¹⁷¹, Y. Ikegami⁶⁸, M. Ikeno⁶⁸, Y. Ilchenko^{11,v}, D. Iliadis¹⁵⁵, N. Ilic¹⁴⁴,
 T. Ince¹⁰², G. Introzzi^{122a,122b}, P. Ioannou^{9,*}, M. Iodice^{135a}, K. Iordanidou³⁷, V. Ippolito⁵⁹, M. Ishino⁷⁰,
 M. Ishitsuka¹⁵⁸, R. Ishmukhametov¹¹², C. Issever¹²¹, S. Isti^{20a}, F. Ito¹⁶¹, J.M. Iturbe Ponce⁸⁶,
 R. Iuppa^{134a,134b}, W. Iwanski⁴¹, H. Iwasaki⁶⁸, J.M. Izen⁴³, V. Izzo^{105a}, S. Jabbar³, B. Jackson¹²³,
 M. Jackson⁷⁶, P. Jackson¹, V. Jain², K.B. Jakobi⁸⁵, K. Jakobs⁵⁰, S. Jakobsen³², T. Jakoubek¹²⁸,
 D.O. Jamin¹¹⁵, D.K. Jana⁸¹, E. Jansen⁸⁰, R. Jansky⁶⁴, J. Janssen²³, M. Janus⁵⁶, G. Jarlskog⁸³,
 N. Javadov^{67,b}, T. Javůrek⁵⁰, F. Jeanneau¹³⁷, L. Jeanty¹⁶, J. Jejelava^{53a,w}, G.-Y. Jeng¹⁵¹, D. Jennens⁹⁰,
 P. Jenni^{50,x}, J. Jentzsch⁴⁵, C. Jeske¹⁷⁰, S. Jézéquel⁵, H. Ji¹⁷³, J. Jia¹⁴⁹, H. Jiang⁶⁶, Y. Jiang^{35b},
 S. Jiggins⁸⁰, J. Jimenez Pena¹⁶⁷, S. Jin^{35a}, A. Jinaru^{28b}, O. Jinnouchi¹⁵⁸, P. Johansson¹⁴⁰, K.A. Johns⁷,
 W.J. Johnson¹³⁹, K. Jon-And^{147a,147b}, G. Jones¹⁷⁰, R.W.L. Jones⁷⁴, S. Jones⁷, T.J. Jones⁷⁶,
 J. Jongmanns^{60a}, P.M. Jorge^{127a,127b}, J. Jovicevic^{160a}, X. Ju¹⁷³, A. Juste Rozas^{13,r}, M.K. Köhler¹⁷²,
 A. Kaczmarska⁴¹, M. Kado¹¹⁸, H. Kagan¹¹², M. Kagan¹⁴⁴, S.J. Kahn⁸⁷, E. Kajomovitz⁴⁷,
 C.W. Kalderon¹²¹, A. Kaluza⁸⁵, S. Kama⁴², A. Kamenshchikov¹³¹, N. Kanaya¹⁵⁶, S. Kaneti³⁰,
 L. Kanjur⁷⁷, V.A. Kantserov⁹⁹, J. Kanzaki⁶⁸, B. Kaplan¹¹¹, L.S. Kaplan¹⁷³, A. Kapliy³³, D. Kar^{146c},
 K. Karakostas¹⁰, A. Karamaoun³, N. Karastathis¹⁰, M.J. Kareem⁵⁶, E. Karentzos¹⁰, M. Karnevskiy⁸⁵,
 S.N. Karpov⁶⁷, Z.M. Karpova⁶⁷, K. Karthik¹¹¹, V. Kartvelishvili⁷⁴, A.N. Karyukhin¹³¹, K. Kasahara¹⁶¹,
 L. Kashif¹⁷³, R.D. Kass¹¹², A. Kastanas¹⁵, Y. Kataoka¹⁵⁶, C. Kato¹⁵⁶, A. Katre⁵¹, J. Katzy⁴⁴,
 K. Kawagoe⁷², T. Kawamoto¹⁵⁶, G. Kawamura⁵⁶, S. Kazama¹⁵⁶, V.F. Kazanin^{110,c}, R. Keeler¹⁶⁹,
 R. Kehoe⁴², J.S. Keller⁴⁴, J.J. Kempster⁷⁹, K Kentaro¹⁰⁴, H. Keoshkerian¹⁵⁹, O. Kepka¹²⁸,
 B.P. Kerševan⁷⁷, S. Kersten¹⁷⁵, R.A. Keyes⁸⁹, F. Khalil-zada¹², A. Khanov¹¹⁵, A.G. Kharlamov^{110,c},
 T.J. Khoo⁵¹, V. Khovanskiy⁹⁸, E. Khramov⁶⁷, J. Khubua^{53b,y}, S. Kido⁶⁹, H.Y. Kim⁸, S.H. Kim¹⁶¹,
 Y.K. Kim³³, N. Kimura¹⁵⁵, O.M. Kind¹⁷, B.T. King⁷⁶, M. King¹⁶⁷, S.B. King¹⁶⁸, J. Kirk¹³²,
 A.E. Kiryunin¹⁰², T. Kishimoto⁶⁹, D. Kisielewska^{40a}, F. Kiss⁵⁰, K. Kiuchi¹⁶¹, O. Kivernyk¹³⁷,
 E. Kladiva^{145b}, M.H. Klein³⁷, M. Klein⁷⁶, U. Klein⁷⁶, K. Kleinknecht⁸⁵, P. Klimek^{147a,147b},
 A. Klimentov²⁷, R. Klingenberg⁴⁵, J.A. Klinger¹⁴⁰, T. Klioutchnikova³², E.-E. Kluge^{60a}, P. Kluit¹⁰⁸,
 S. Kluth¹⁰², J. Knapik⁴¹, E. Kneringer⁶⁴, E.B.F.G. Knoops⁸⁷, A. Knue⁵⁵, A. Kobayashi¹⁵⁶,
 D. Kobayashi¹⁵⁸, T. Kobayashi¹⁵⁶, M. Kobel⁴⁶, M. Kocian¹⁴⁴, P. Kodys¹³⁰, T. Koffas³¹, E. Koffeman¹⁰⁸,
 T. Koi¹⁴⁴, H. Kolanoski¹⁷, M. Kolb^{60b}, I. Koletsou⁵, A.A. Komar^{97,*}, Y. Komori¹⁵⁶, T. Kondo⁶⁸,
 N. Kondrashova⁴⁴, K. Köneke⁵⁰, A.C. König¹⁰⁷, T. Kono^{68,z}, R. Konoplich^{111,aa}, N. Konstantinidis⁸⁰,
 R. Kopeliansky⁶³, S. Koperny^{40a}, L. Köpke⁸⁵, A.K. Kopp⁵⁰, K. Korcyl⁴¹, K. Kordas¹⁵⁵, A. Korn⁸⁰,
 A.A. Korol^{110,c}, I. Korolkov¹³, E.V. Korolkova¹⁴⁰, O. Kortner¹⁰², S. Kortner¹⁰², T. Kosek¹³⁰,
 V.V. Kostyukhin²³, A. Kotwal⁴⁷, A. Kourkoumeli-Charalampidi¹⁵⁵, C. Kourkoumelis⁹, V. Kouskoura²⁷,
 A.B. Kowalewska⁴¹, R. Kowalewski¹⁶⁹, T.Z. Kowalski^{40a}, C. Kozakai¹⁵⁶, W. Kozanecki¹³⁷,
 A.S. Kozhin¹³¹, V.A. Kramarenko¹⁰⁰, G. Kramberger⁷⁷, D. Krasnopovertsev⁹⁹, M.W. Krasny⁸²,
 A. Krasznahorkay³², J.K. Kraus²³, A. Kravchenko²⁷, M. Kretz^{60c}, J. Kretzscher⁷⁶, K. Kreutzfeldt⁵⁴,
 P. Krieger¹⁵⁹, K. Krizka³³, K. Kroeninger⁴⁵, H. Kroha¹⁰², J. Kroll¹²³, J. Kroeseberg²³, J. Krstic¹⁴,
 U. Kruchonak⁶⁷, H. Krüger²³, N. Krumnack⁶⁶, A. Kruse¹⁷³, M.C. Kruse⁴⁷, M. Kruskal²⁴, T. Kubota⁹⁰,
 H. Kucuk⁸⁰, S. Kuday^{4b}, J.T. Kuechler¹⁷⁵, S. Kuehn⁵⁰, A. Kugel^{60c}, F. Kuger¹⁷⁴, A. Kuhl¹³⁸, T. Kuhl⁴⁴,
 V. Kukhtin⁶⁷, R. Kukla¹³⁷, Y. Kulchitsky⁹⁴, S. Kuleshov^{34b}, M. Kuna^{133a,133b}, T. Kunigo⁷⁰, A. Kupco¹²⁸,
 H. Kurashige⁶⁹, Y.A. Kurochkin⁹⁴, V. Kus¹²⁸, E.S. Kuwertz¹⁶⁹, M. Kuze¹⁵⁸, J. Kvita¹¹⁶, T. Kwan¹⁶⁹,
 D. Kyriazopoulos¹⁴⁰, A. La Rosa¹⁰², J.L. La Rosa Navarro^{26d}, L. La Rotonda^{39a,39b}, C. Lacasta¹⁶⁷,
 F. Lacava^{133a,133b}, J. Lacey³¹, H. Lacker¹⁷, D. Lacour⁸², V.R. Lacuesta¹⁶⁷, E. Ladygin⁶⁷, R. Lafaye⁵,
 B. Laforge⁸², T. Lagouri¹⁷⁶, S. Lai⁵⁶, S. Lammers⁶³, W. Lampl⁷, E. Lançon¹³⁷, U. Landgraf⁵⁰,
 M.P.J. Landon⁷⁸, V.S. Lang^{60a}, J.C. Lange¹³, A.J. Lankford¹⁶³, F. Lanni²⁷, K. Lantzsch²³, A. Lanza^{122a},
 S. Laplace⁸², C. Lapoire³², J.F. Laporte¹³⁷, T. Lari^{93a}, F. Lasagni Manghi^{22a,22b}, M. Lassnig³²,
 P. Laurelli⁴⁹, W. Lavrijssen¹⁶, A.T. Law¹³⁸, P. Laycock⁷⁶, T. Lazovich⁵⁹, M. Lazzaroni^{93a,93b}, B. Le⁹⁰,

O. Le Dertz⁸², E. Le Guiriec⁸⁷, E.P. Le Quilleuc¹³⁷, M. LeBlanc¹⁶⁹, T. LeCompte⁶,
 F. Ledroit-Guillon⁵⁷, C.A. Lee²⁷, S.C. Lee¹⁵², L. Lee¹, G. Lefebvre⁸², M. Lefebvre¹⁶⁹, F. Legger¹⁰¹,
 C. Leggett¹⁶, A. Lehan⁷⁶, G. Lehmann Miotto³², X. Lei⁷, W.A. Leight³¹, A. Leisos^{155,ab},
 A.G. Leister¹⁷⁶, M.A.L. Leite^{26d}, R. Leitner¹³⁰, D. Lellouch¹⁷², B. Lemmer⁵⁶, K.J.C. Leney⁸⁰, T. Lenz²³,
 B. Lenzi³², R. Leone⁷, S. Leone^{125a,125b}, C. Leonidopoulos⁴⁸, S. Leontsinis¹⁰, G. Lerner¹⁵⁰, C. Leroy⁹⁶,
 A.A.J. Lesage¹³⁷, C.G. Lester³⁰, M. Levchenko¹²⁴, J. Levêque⁵, D. Levin⁹¹, L.J. Levinson¹⁷²,
 M. Levy¹⁹, D. Lewis⁷⁸, A.M. Leyko²³, M. Leyton⁴³, B. Li^{35b,o}, H. Li¹⁴⁹, H.L. Li³³, L. Li⁴⁷, L. Li^{35e},
 Q. Li^{35a}, S. Li⁴⁷, X. Li⁸⁶, Y. Li¹⁴², Z. Liang^{35a}, B. Liberti^{134a}, A. Liblong¹⁵⁹, P. Lichard³², K. Lie¹⁶⁶,
 J. Liebal²³, W. Liebig¹⁵, A. Limosani¹⁵¹, S.C. Lin^{152,ac}, T.H. Lin⁸⁵, B.E. Lindquist¹⁴⁹, A.E. Lionti⁵¹,
 E. Lipeles¹²³, A. Lipniacka¹⁵, M. Lisovyi^{60b}, T.M. Liss¹⁶⁶, A. Lister¹⁶⁸, A.M. Litke¹³⁸, B. Liu^{152,ad},
 D. Liu¹⁵², H. Liu⁹¹, H. Liu²⁷, J. Liu⁸⁷, J.B. Liu^{35b}, K. Liu⁸⁷, L. Liu¹⁶⁶, M. Liu⁴⁷, M. Liu^{35b}, Y.L. Liu^{35b},
 Y. Liu^{35b}, M. Livan^{122a,122b}, A. Lleres⁵⁷, J. Llorente Merino^{35a}, S.L. Lloyd⁷⁸, F. Lo Sterzo¹⁵²,
 E. Lobodzinska⁴⁴, P. Loch⁷, W.S. Lockman¹³⁸, F.K. Loebinger⁸⁶, A.E. Loevschall-Jensen³⁸,
 K.M. Loew²⁵, A. Loginov¹⁷⁶, T. Lohse¹⁷, K. Lohwasser⁴⁴, M. Lokajicek¹²⁸, B.A. Long²⁴, J.D. Long¹⁶⁶,
 R.E. Long⁷⁴, L. Longo^{75a,75b}, K.A.Looper¹¹², L. Lopes^{127a}, D. Lopez Mateos⁵⁹, B. Lopez Paredes¹⁴⁰,
 I. Lopez Paz¹³, A. Lopez Solis⁸², J. Lorenz¹⁰¹, N. Lorenzo Martinez⁶³, M. Losada²¹, P.J. Lösel¹⁰¹,
 X. Lou^{35a}, A. Lounis¹¹⁸, J. Love⁶, P.A. Love⁷⁴, H. Lu^{62a}, N. Lu⁹¹, H.J. Lubatti¹³⁹, C. Luci^{133a,133b},
 A. Lucotte⁵⁷, C. Luedtke⁵⁰, F. Luehring⁶³, W. Lukas⁶⁴, L. Luminari^{133a}, O. Lundberg^{147a,147b},
 B. Lund-Jensen¹⁴⁸, P.M. Luzi⁸², D. Lynn²⁷, R. Lysak¹²⁸, E. Lytken⁸³, V. Lyubushkin⁶⁷, H. Ma²⁷,
 L.L. Ma^{35d}, Y. Ma^{35d}, G. Maccarrone⁴⁹, A. Macchiolo¹⁰², C.M. Macdonald¹⁴⁰, B. Maček⁷⁷,
 J. Machado Miguens^{123,127b}, D. Madaffari⁸⁷, R. Madar³⁶, H.J. Maddocks¹⁶⁵, W.F. Mader⁴⁶,
 A. Madsen⁴⁴, J. Maeda⁶⁹, S. Maeland¹⁵, T. Maeno²⁷, A. Maevskiy¹⁰⁰, E. Magradze⁵⁶, J. Mahlstedt¹⁰⁸,
 C. Maiani¹¹⁸, C. Maidantchik^{26a}, A.A. Maier¹⁰², T. Maier¹⁰¹, A. Maio^{127a,127b,127d}, S. Majewski¹¹⁷,
 Y. Makida⁶⁸, N. Makovec¹¹⁸, B. Malaescu⁸², Pa. Malecki⁴¹, V.P. Maleev¹²⁴, F. Malek⁵⁷, U. Mallik⁶⁵,
 D. Malon⁶, C. Malone¹⁴⁴, S. Maltezos¹⁰, S. Malyukov³², J. Mamuzic¹⁶⁷, G. Mancini⁴⁹, B. Mandelli³²,
 L. Mandelli^{93a}, I. Mandić⁷⁷, J. Maneira^{127a,127b}, L. Manhaes de Andrade Filho^{26b},
 J. Manjarres Ramos^{160b}, A. Mann¹⁰¹, A. Manousos³², B. Mansoulie¹³⁷, J.D. Mansour^{35a}, R. Mantifel⁸⁹,
 M. Mantoani⁵⁶, S. Manzoni^{93a,93b}, L. Mapelli³², G. Marceca²⁹, L. March⁵¹, G. Marchiori⁸²,
 M. Marcisovsky¹²⁸, M. Marjanovic¹⁴, D.E. Marley⁹¹, F. Marroquim^{26a}, S.P. Marsden⁸⁶, Z. Marshall¹⁶,
 S. Marti-Garcia¹⁶⁷, B. Martin⁹², T.A. Martin¹⁷⁰, V.J. Martin⁴⁸, B. Martin dit Latour¹⁵, M. Martinez^{13,r},
 S. Martin-Haugh¹³², V.S. Martoiu^{28b}, A.C. Martyniuk⁸⁰, M. Marx¹³⁹, A. Marzin³², L. Masetti⁸⁵,
 T. Mashimo¹⁵⁶, R. Mashinistov⁹⁷, J. Masik⁸⁶, A.L. Maslennikov^{110,c}, I. Massa^{22a,22b}, L. Massa^{22a,22b},
 P. Mastrandrea⁵, A. Mastroberardino^{39a,39b}, T. Masubuchi¹⁵⁶, P. Mättig¹⁷⁵, J. Mattmann⁸⁵, J. Maurer^{28b},
 S.J. Maxfield⁷⁶, D.A. Maximov^{110,c}, R. Mazini¹⁵², S.M. Mazza^{93a,93b}, N.C. Mc Fadden¹⁰⁶,
 G. Mc Goldrick¹⁵⁹, S.P. Mc Kee⁹¹, A. McCarn⁹¹, R.L. McCarthy¹⁴⁹, T.G. McCarthy¹⁰²,
 L.I. McClymont⁸⁰, E.F. McDonald⁹⁰, K.W. McFarlane^{58,*}, J.A. McFayden⁸⁰, G. McHedlidze⁵⁶,
 S.J. McMahon¹³², R.A. McPherson^{169,l}, M. Medinnis⁴⁴, S. Meehan¹³⁹, S. Mehlhase¹⁰¹, A. Mehta⁷⁶,
 K. Meier^{60a}, C. Meineck¹⁰¹, B. Meirose⁴³, D. Melini¹⁶⁷, B.R. Mellado Garcia^{146c}, M. Melo^{145a},
 F. Meloni¹⁸, A. Mengarelli^{22a,22b}, S. Menke¹⁰², E. Meoni¹⁶², S. Mergelmeyer¹⁷, P. Mermod⁵¹,
 L. Merola^{105a,105b}, C. Meroni^{93a}, F.S. Merritt³³, A. Messina^{133a,133b}, J. Metcalfe⁶, A.S. Mete¹⁶³,
 C. Meyer⁸⁵, C. Meyer¹²³, J.-P. Meyer¹³⁷, J. Meyer¹⁰⁸, H. Meyer Zu Theenhausen^{60a}, F. Miano¹⁵⁰,
 R.P. Middleton¹³², S. Miglioranzi^{52a,52b}, L. Mijović²³, G. Mikenberg¹⁷², M. Mikestikova¹²⁸,
 M. Mikuž⁷⁷, M. Milesi⁹⁰, A. Milic⁶⁴, D.W. Miller³³, C. Mills⁴⁸, A. Milov¹⁷², D.A. Milstead^{147a,147b},
 A.A. Minaenko¹³¹, Y. Minami¹⁵⁶, I.A. Minashvili⁶⁷, A.I. Mincer¹¹¹, B. Mindur^{40a}, M. Mineev⁶⁷,
 Y. Ming¹⁷³, L.M. Mir¹³, K.P. Mistry¹²³, T. Mitani¹⁷¹, J. Mitrevski¹⁰¹, V.A. Mitsou¹⁶⁷, A. Miucci⁵¹,
 P.S. Miyagawa¹⁴⁰, J.U. Mjörnmark⁸³, T. Moa^{147a,147b}, K. Mochizuki⁹⁶, S. Mohapatra³⁷,
 S. Molander^{147a,147b}, R. Moles-Valls²³, R. Monden⁷⁰, M.C. Mondragon⁹², K. Mönig⁴⁴, J. Monk³⁸,

E. Monnier⁸⁷, A. Montalbano¹⁴⁹, J. Montejo Berlingen³², F. Monticelli⁷³, S. Monzani^{93a,93b},
 R.W. Moore³, N. Morange¹¹⁸, D. Moreno²¹, M. Moreno Llácer⁵⁶, P. Morettini^{52a}, D. Mori¹⁴³,
 T. Mori¹⁵⁶, M. Morii⁵⁹, M. Morinaga¹⁵⁶, V. Morisbak¹²⁰, S. Moritz⁸⁵, A.K. Morley¹⁵¹, G. Mornacchi³²,
 J.D. Morris⁷⁸, S.S. Mortensen³⁸, L. Morvaj¹⁴⁹, M. Mosidze^{53b}, J. Moss¹⁴⁴, K. Motohashi¹⁵⁸,
 R. Mount¹⁴⁴, E. Mountricha²⁷, S.V. Mouraviev^{97,*}, E.J.W. Moyse⁸⁸, S. Muanza⁸⁷, R.D. Mudd¹⁹,
 F. Mueller¹⁰², J. Mueller¹²⁶, R.S.P. Mueller¹⁰¹, T. Mueller³⁰, D. Muenstermann⁷⁴, P. Mullen⁵⁵,
 G.A. Mullier¹⁸, F.J. Munoz Sanchez⁸⁶, J.A. Murillo Quijada¹⁹, W.J. Murray^{170,132}, H. Musheghyan⁵⁶,
 M. Muškinja⁷⁷, A.G. Myagkov^{131,ae}, M. Myska¹²⁹, B.P. Nachman¹⁴⁴, O. Nackenhorst⁵¹, K. Nagai¹²¹,
 R. Nagai^{68,z}, K. Nagano⁶⁸, Y. Nagasaka⁶¹, K. Nagata¹⁶¹, M. Nagel⁵⁰, E. Nagy⁸⁷, A.M. Nairz³²,
 Y. Nakahama³², K. Nakamura⁶⁸, T. Nakamura¹⁵⁶, I. Nakano¹¹³, H. Namasivayam⁴³,
 R.F. Naranjo Garcia⁴⁴, R. Narayan¹¹, D.I. Narrias Villar^{60a}, I. Naryshkin¹²⁴, T. Naumann⁴⁴,
 G. Navarro²¹, R. Nayyar⁷, H.A. Neal⁹¹, P.Yu. Nechaeva⁹⁷, T.J. Neep⁸⁶, P.D. Nef¹⁴⁴, A. Negri^{122a,122b},
 M. Negrini^{22a}, S. Nektarijevic¹⁰⁷, C. Nellist¹¹⁸, A. Nelson¹⁶³, S. Nemecek¹²⁸, P. Nemethy¹¹¹,
 A.A. Nepomuceno^{26a}, M. Nessi^{32,af}, M.S. Neubauer¹⁶⁶, M. Neumann¹⁷⁵, R.M. Neves¹¹¹, P. Nevski²⁷,
 P.R. Newman¹⁹, D.H. Nguyen⁶, T. Nguyen Manh⁹⁶, R.B. Nickerson¹²¹, R. Nicolaïdou¹³⁷, J. Nielsen¹³⁸,
 A. Nikiforov¹⁷, V. Nikolaenko^{131,ae}, I. Nikolic-Audit⁸², K. Nikolopoulos¹⁹, J.K. Nilsen¹²⁰, P. Nilsson²⁷,
 Y. Ninomiya¹⁵⁶, A. Nisati^{133a}, R. Nisius¹⁰², T. Nobe¹⁵⁶, L. Nodulman⁶, M. Nomachi¹¹⁹, I. Nomidis³¹,
 T. Nooney⁷⁸, S. Norberg¹¹⁴, M. Nordberg³², N. Norjoharuddeen¹²¹, O. Novgorodova⁴⁶, S. Nowak¹⁰²,
 M. Nozaki⁶⁸, L. Nozka¹¹⁶, K. Ntekas¹⁰, E. Nurse⁸⁰, F. Nuti⁹⁰, F. O'grady⁷, D.C. O'Neil¹⁴³,
 A.A. O'Rourke⁴⁴, V. O'Shea⁵⁵, F.G. Oakham^{31,d}, H. Oberlack¹⁰², T. Obermann²³, J. Ocariz⁸²,
 A. Ochi⁶⁹, I. Ochoa³⁷, J.P. Ochoa-Ricoux^{34a}, S. Oda⁷², S. Odaka⁶⁸, H. Ogren⁶³, A. Oh⁸⁶, S.H. Oh⁴⁷,
 C.C. Ohm¹⁶, H. Ohman¹⁶⁵, H. Oide³², H. Okawa¹⁶¹, Y. Okumura³³, T. Okuyama⁶⁸, A. Olariu^{28b},
 L.F. Oleiro Seabra^{127a}, S.A. Olivares Pino⁴⁸, D. Oliveira Damazio²⁷, A. Olszewski⁴¹, J. Olszowska⁴¹,
 A. Onofre^{127a,127e}, K. Onogi¹⁰⁴, P.U.E. Onyisi^{11,v}, M.J. Oreglia³³, Y. Oren¹⁵⁴, D. Orestano^{135a,135b},
 N. Orlando^{62b}, R.S. Orr¹⁵⁹, B. Osculati^{52a,52b}, R. Ospanov⁸⁶, G. Otero y Garzon²⁹, H. Otono⁷²,
 M. Ouchrif^{136d}, F. Ould-Saada¹²⁰, A. Ouraou¹³⁷, K.P. Oussoren¹⁰⁸, Q. Ouyang^{35a}, M. Owen⁵⁵,
 R.E. Owen¹⁹, V.E. Ozcan^{20a}, N. Ozturk⁸, K. Pachal¹⁴³, A. Pacheco Pages¹³, L. Pacheco Rodriguez¹³⁷,
 C. Padilla Aranda¹³, M. Pagáčová⁵⁰, S. Pagan Griso¹⁶, F. Paige²⁷, P. Pais⁸⁸, K. Pajchel¹²⁰,
 G. Palacino^{160b}, S. Palestini³², M. Palka^{40b}, D. Pallin³⁶, A. Palma^{127a,127b}, E.St. Panagiotopoulou¹⁰,
 C.E. Pandini⁸², J.G. Panduro Vazquez⁷⁹, P. Pani^{147a,147b}, S. Panitkin²⁷, D. Pantea^{28b}, L. Paolozzi⁵¹,
 Th.D. Papadopoulou¹⁰, K. Papageorgiou¹⁵⁵, A. Paramonov⁶, D. Paredes Hernandez¹⁷⁶, A.J. Parker⁷⁴,
 M.A. Parker³⁰, K.A. Parker¹⁴⁰, F. Parodi^{52a,52b}, J.A. Parsons³⁷, U. Parzefall⁵⁰, V.R. Pascuzzi¹⁵⁹,
 E. Pasqualucci^{133a}, S. Passaggio^{52a}, Fr. Pastore⁷⁹, G. Pásztor^{31,ag}, S. Pataraia¹⁷⁵, J.R. Pater⁸⁶, T. Pauly³²,
 J. Pearce¹⁶⁹, B. Pearson¹¹⁴, L.E. Pedersen³⁸, M. Pedersen¹²⁰, S. Pedraza Lopez¹⁶⁷, R. Pedro^{127a,127b},
 S.V. Peleganchuk^{110,c}, D. Pelikan¹⁶⁵, O. Penc¹²⁸, C. Peng^{35a}, H. Peng^{35b}, J. Penwell⁶³, B.S. Peralva^{26b},
 M.M. Perego¹³⁷, D.V. Perepelitsa²⁷, E. Perez Codina^{160a}, L. Perini^{93a,93b}, H. Pernegger³²,
 S. Perrella^{105a,105b}, R. Peschke⁴⁴, V.D. Peshekhanov⁶⁷, K. Peters⁴⁴, R.F.Y. Peters⁸⁶, B.A. Petersen³²,
 T.C. Petersen³⁸, E. Petit⁵⁷, A. Petridis¹, C. Petridou¹⁵⁵, P. Petroff¹¹⁸, E. Petrolo^{133a}, M. Petrov¹²¹,
 F. Petrucci^{135a,135b}, N.E. Pettersson⁸⁸, A. Peyaud¹³⁷, R. Pezoa^{34b}, P.W. Phillips¹³², G. Piacquadio¹⁴⁴,
 E. Pianori¹⁷⁰, A. Picazio⁸⁸, E. Piccaro⁷⁸, M. Piccinini^{22a,22b}, M.A. Pickering¹²¹, R. Piegaia²⁹,
 J.E. Pilcher³³, A.D. Pilkington⁸⁶, A.W.J. Pin⁸⁶, M. Pinamonti^{164a,164c,ah}, J.L. Pinfold³, A. Pingel³⁸,
 S. Pires⁸², H. Pirumov⁴⁴, M. Pitt¹⁷², L. Plazak^{145a}, M.-A. Pleier²⁷, V. Pleskot⁸⁵, E. Plotnikova⁶⁷,
 P. Plucinski⁹², D. Pluth⁶⁶, R. Poettgen^{147a,147b}, L. Poggioli¹¹⁸, D. Pohl²³, G. Polesello^{122a}, A. Poley⁴⁴,
 A. Pollicchio^{39a,39b}, R. Polifka¹⁵⁹, A. Polini^{22a}, C.S. Pollard⁵⁵, V. Polychronakos²⁷, K. Pommès³²,
 L. Pontecorvo^{133a}, B.G. Pope⁹², G.A. Popeneciu^{28c}, D.S. Popovic¹⁴, A. Poppleton³², S. Pospisil¹²⁹,
 K. Potamianos¹⁶, I.N. Potrap⁶⁷, C.J. Potter³⁰, C.T. Potter¹¹⁷, G. Pouillard³², J. Poveda³²,
 V. Pozdnyakov⁶⁷, M.E. Pozo Astigarraga³², P. Pralavorio⁸⁷, A. Pranko¹⁶, S. Prell⁶⁶, D. Price⁸⁶,

L.E. Price⁶, M. Primavera^{75a}, S. Prince⁸⁹, M. Proissl⁴⁸, K. Prokofiev^{62c}, F. Prokoshin^{34b},
 S. Protopopescu²⁷, J. Proudfoot⁶, M. Przybycien^{40a}, D. Puddu^{135a,135b}, M. Purohit^{27,ai}, P. Puzo¹¹⁸,
 J. Qian⁹¹, G. Qin⁵⁵, Y. Qin⁸⁶, A. Quadt⁵⁶, W.B. Quayle^{164a,164b}, M. Queitsch-Maitland⁸⁶, D. Quilty⁵⁵,
 S. Raddum¹²⁰, V. Radeka²⁷, V. Radescu^{60b}, S.K. Radhakrishnan¹⁴⁹, P. Radloff¹¹⁷, P. Rados⁹⁰,
 F. Ragusa^{93a,93b}, G. Rahal¹⁷⁸, J.A. Raine⁸⁶, S. Rajagopalan²⁷, M. Rammensee³², C. Rangel-Smith¹⁶⁵,
 M.G. Ratti^{93a,93b}, F. Rauscher¹⁰¹, S. Rave⁸⁵, T. Ravenscroft⁵⁵, I. Ravinovich¹⁷², M. Raymond³²,
 A.L. Read¹²⁰, N.P. Readioff⁷⁶, M. Reale^{75a,75b}, D.M. Rebuzzi^{122a,122b}, A. Redelbach¹⁷⁴, G. Redlinger²⁷,
 R. Reece¹³⁸, K. Reeves⁴³, L. Rehnisch¹⁷, J. Reichert¹²³, H. Reisin²⁹, C. Rembsler³², H. Ren^{35a},
 M. Rescigno^{133a}, S. Resconi^{93a}, O.L. Rezanova^{110,c}, P. Reznicek¹³⁰, R. Rezvani⁹⁶, R. Richter¹⁰²,
 S. Richter⁸⁰, E. Richter-Was^{40b}, O. Ricken²³, M. Ridel⁸², P. Rieck¹⁷, C.J. Riegel¹⁷⁵, J. Rieger⁵⁶,
 O. Rifki¹¹⁴, M. Rijssenbeek¹⁴⁹, A. Rimoldi^{122a,122b}, M. Rimoldi¹⁸, L. Rinaldi^{22a}, B. Ristic⁵¹, E. Ritsch³²,
 I. Riu¹³, F. Rizatdinova¹¹⁵, E. Rizvi⁷⁸, C. Rizzi¹³, S.H. Robertson^{89,l}, A. Robichaud-Veronneau⁸⁹,
 D. Robinson³⁰, J.E.M. Robinson⁴⁴, A. Robson⁵⁵, C. Roda^{125a,125b}, Y. Rodina⁸⁷, A. Rodriguez Perez¹³,
 D. Rodriguez Rodriguez¹⁶⁷, S. Roe³², C.S. Rogan⁵⁹, O. Røhne¹²⁰, A. Romaniouk⁹⁹, M. Romano^{22a,22b},
 S.M. Romano Saez³⁶, E. Romero Adam¹⁶⁷, N. Rompotis¹³⁹, M. Ronzani⁵⁰, L. Roos⁸², E. Ros¹⁶⁷,
 S. Rosati^{133a}, K. Rosbach⁵⁰, P. Rose¹³⁸, O. Rosenthal¹⁴², N.-A. Rosien⁵⁶, V. Rossetti^{147a,147b},
 E. Rossi^{105a,105b}, L.P. Rossi^{52a}, J.H.N. Rosten³⁰, R. Rosten¹³⁹, M. Rotaru^{28b}, I. Roth¹⁷², J. Rothberg¹³⁹,
 D. Rousseau¹¹⁸, C.R. Royon¹³⁷, A. Rozanov⁸⁷, Y. Rozen¹⁵³, X. Ruan^{146c}, F. Rubbo¹⁴⁴,
 M.S. Rudolph¹⁵⁹, F. Rühr⁵⁰, A. Ruiz-Martinez³¹, Z. Rurikova⁵⁰, N.A. Rusakovich⁶⁷, A. Ruschke¹⁰¹,
 H.L. Russell¹³⁹, J.P. Rutherford⁷, N. Ruthmann³², Y.F. Ryabov¹²⁴, M. Rybar¹⁶⁶, G. Rybkin¹¹⁸, S. Ryu⁶,
 A. Ryzhov¹³¹, G.F. Rzehorz⁵⁶, A.F. Saavedra¹⁵¹, G. Sabato¹⁰⁸, S. Sacerdoti²⁹, H.F-W. Sadrozinski¹³⁸,
 R. Sadykov⁶⁷, F. Safai Tehrani^{133a}, P. Saha¹⁰⁹, M. Sahinsoy^{60a}, M. Saimpert¹³⁷, T. Saito¹⁵⁶,
 H. Sakamoto¹⁵⁶, Y. Sakurai¹⁷¹, G. Salamanna^{135a,135b}, A. Salamon^{134a,134b}, J.E. Salazar Loyola^{34b},
 D. Salek¹⁰⁸, P.H. Sales De Bruin¹³⁹, D. Salihagic¹⁰², A. Salnikov¹⁴⁴, J. Salt¹⁶⁷, D. Salvatore^{39a,39b},
 F. Salvatore¹⁵⁰, A. Salvucci^{62a}, A. Salzburger³², D. Sammel⁵⁰, D. Sampsonidis¹⁵⁵, A. Sanchez^{105a,105b},
 J. Sánchez¹⁶⁷, V. Sanchez Martinez¹⁶⁷, H. Sandaker¹²⁰, R.L. Sandbach⁷⁸, H.G. Sander⁸⁵,
 M. Sandhoff¹⁷⁵, C. Sandoval²¹, R. Sandstroem¹⁰², D.P.C. Sankey¹³², M. Sannino^{52a,52b}, A. Sansoni⁴⁹,
 C. Santoni³⁶, R. Santonico^{134a,134b}, H. Santos^{127a}, I. Santoyo Castillo¹⁵⁰, K. Sapp¹²⁶, A. Sapronov⁶⁷,
 J.G. Saraiva^{127a,127d}, B. Sarrazin²³, O. Sasaki⁶⁸, Y. Sasaki¹⁵⁶, K. Sato¹⁶¹, G. Sauvage^{5,*}, E. Sauvan⁵,
 G. Savage⁷⁹, P. Savard^{159,d}, C. Sawyer¹³², L. Sawyer^{81,q}, J. Saxon³³, C. Sbarra^{22a,22b}, A. Sbrizzi^{22a,22b},
 T. Scanlon⁸⁰, D.A. Scannicchio¹⁶³, M. Scarcella¹⁵¹, V. Scarfone^{39a,39b}, J. Schaarschmidt¹⁷²,
 P. Schacht¹⁰², B.M. Schachtner¹⁰¹, D. Schaefer³², R. Schaefer⁴⁴, J. Schaeffer⁸⁵, S. Schaepe²³,
 S. Schaetzel^{60b}, U. Schäfer⁸⁵, A.C. Schaffer¹¹⁸, D. Schaille¹⁰¹, R.D. Schamberger¹⁴⁹, V. Scharf^{60a},
 V.A. Schegelsky¹²⁴, D. Scheirich¹³⁰, M. Schernau¹⁶³, C. Schiavi^{52a,52b}, S. Schier¹³⁸, C. Schillo⁵⁰,
 M. Schioppa^{39a,39b}, S. Schlenker³², K.R. Schmidt-Sommerfeld¹⁰², K. Schmieden³², C. Schmitt⁸⁵,
 S. Schmitt⁴⁴, S. Schmitz⁸⁵, B. Schneider^{160a}, U. Schnoor⁵⁰, L. Schoeffel¹³⁷, A. Schoening^{60b},
 B.D. Schoenrock⁹², E. Schopf²³, M. Schott⁸⁵, J. Schovancova⁸, S. Schramm⁵¹, M. Schreyer¹⁷⁴,
 N. Schuh⁸⁵, M.J. Schultens²³, H.-C. Schultz-Coulon^{60a}, H. Schulz¹⁷, M. Schumacher⁵⁰,
 B.A. Schumm¹³⁸, Ph. Schune¹³⁷, A. Schwartzman¹⁴⁴, T.A. Schwarz⁹¹, Ph. Schwegler¹⁰²,
 H. Schweiger⁸⁶, Ph. Schwemling¹³⁷, R. Schwienhorst⁹², J. Schwindling¹³⁷, T. Schwindt²³, G. Sciolla²⁵,
 F. Scuri^{125a,125b}, F. Scutti⁹⁰, J. Searcy⁹¹, P. Seema²³, S.C. Seidel¹⁰⁶, A. Seiden¹³⁸, F. Seifert¹²⁹,
 J.M. Seixas^{26a}, G. Sekhniaidze^{105a}, K. Sekhon⁹¹, S.J. Sekula⁴², D.M. Seliverstov^{124,*},
 N. Semprini-Cesari^{22a,22b}, C. Serfon¹²⁰, L. Serin¹¹⁸, L. Serkin^{164a,164b}, M. Sessa^{135a,135b}, R. Seuster¹⁶⁹,
 H. Severini¹¹⁴, T. Sfiligoj⁷⁷, F. Sforza³², A. Sfyrla⁵¹, E. Shabalina⁵⁶, N.W. Shaikh^{147a,147b}, L.Y. Shan^{35a},
 R. Shang¹⁶⁶, J.T. Shank²⁴, M. Shapiro¹⁶, P.B. Shatalov⁹⁸, K. Shaw^{164a,164b}, S.M. Shaw⁸⁶,
 A. Shcherbakova^{147a,147b}, C.Y. Shehu¹⁵⁰, P. Sherwood⁸⁰, L. Shi^{152,aj}, S. Shimizu⁶⁹, C.O. Shimmin¹⁶³,
 M. Shimojima¹⁰³, M. Shiyakova^{67,ak}, A. Shmeleva⁹⁷, D. Shoaleh Saadi⁹⁶, M.J. Shochet³³,

S. Shojaii^{93a,93b}, S. Shrestha¹¹², E. Shulga⁹⁹, M.A. Shupe⁷, P. Sicho¹²⁸, A.M. Sickles¹⁶⁶, P.E. Sidebo¹⁴⁸, O. Sidiropoulou¹⁷⁴, D. Sidorov¹¹⁵, A. Sidoti^{22a,22b}, F. Siegert⁴⁶, Dj. Sijacki¹⁴, J. Silva^{127a,127d}, S.B. Silverstein^{147a}, V. Simak¹²⁹, O. Simard⁵, Lj. Simic¹⁴, S. Simion¹¹⁸, E. Simioni⁸⁵, B. Simmons⁸⁰, D. Simon³⁶, M. Simon⁸⁵, P. Sinervo¹⁵⁹, N.B. Sinev¹¹⁷, M. Sioli^{22a,22b}, G. Siragusa¹⁷⁴, S.Yu. Sivoklokov¹⁰⁰, J. Sjölin^{147a,147b}, T.B. Sjursen¹⁵, M.B. Skinner⁷⁴, H.P. Skottowe⁵⁹, P. Skubic¹¹⁴, M. Slater¹⁹, T. Slavicek¹²⁹, M. Slawinska¹⁰⁸, K. Sliwa¹⁶², R. Slovak¹³⁰, V. Smakhtin¹⁷², B.H. Smart⁵, L. Smestad¹⁵, J. Smiesko^{145a}, S.Yu. Smirnov⁹⁹, Y. Smirnov⁹⁹, L.N. Smirnova^{100,al}, O. Smirnova⁸³, M.N.K. Smith³⁷, R.W. Smith³⁷, M. Smizanska⁷⁴, K. Smolek¹²⁹, A.A. Snesarev⁹⁷, S. Snyder²⁷, R. Sobie^{169,l}, F. Socher⁴⁶, A. Soffer¹⁵⁴, D.A. Soh¹⁵², G. Sokhrannyi⁷⁷, C.A. Solans Sanchez³², M. Solar¹²⁹, E.Yu. Soldatov⁹⁹, U. Soldevila¹⁶⁷, A.A. Solodkov¹³¹, A. Soloshenko⁶⁷, O.V. Solovyanov¹³¹, V. Solovyev¹²⁴, P. Sommer⁵⁰, H. Son¹⁶², H.Y. Song^{35b,am}, A. Sood¹⁶, A. Sopczak¹²⁹, V. Sopko¹²⁹, V. Sorin¹³, D. Sosa^{60b}, C.L. Sotiropoulou^{125a,125b}, R. Soualah^{164a,164c}, A.M. Soukharev^{110,c}, D. South⁴⁴, B.C. Sowden⁷⁹, S. Spagnolo^{75a,75b}, M. Spalla^{125a,125b}, M. Spangenberg¹⁷⁰, F. Spanò⁷⁹, D. Sperlich¹⁷, F. Spettel¹⁰², R. Spighi^{22a}, G. Spigo³², L.A. Spiller⁹⁰, M. Spousta¹³⁰, R.D. St. Denis^{55,*}, A. Stabile^{93a}, R. Stamen^{60a}, S. Stamm¹⁷, E. Stanecka⁴¹, R.W. Stanek⁶, C. Stanescu^{135a}, M. Stanescu-Bellu⁴⁴, M.M. Stanitzki⁴⁴, S. Stapnes¹²⁰, E.A. Starchenko¹³¹, G.H. Stark³³, J. Stark⁵⁷, P. Staroba¹²⁸, P. Starovoitov^{60a}, S. Stärz³², R. Staszewski⁴¹, P. Steinberg²⁷, B. Stelzer¹⁴³, H.J. Stelzer³², O. Stelzer-Chilton^{160a}, H. Stenzel⁵⁴, G.A. Stewart⁵⁵, J.A. Stillings²³, M.C. Stockton⁸⁹, M. Stoebe⁸⁹, G. Stoica^{28b}, P. Stolte⁵⁶, S. Stonjek¹⁰², A.R. Stradling⁸, A. Straessner⁴⁶, M.E. Stramaglia¹⁸, J. Strandberg¹⁴⁸, S. Strandberg^{147a,147b}, A. Strandlie¹²⁰, M. Strauss¹¹⁴, P. Strizenec^{145b}, R. Ströhmer¹⁷⁴, D.M. Strom¹¹⁷, R. Stroynowski⁴², A. Strubig¹⁰⁷, S.A. Stucci¹⁸, B. Stugu¹⁵, N.A. Styles⁴⁴, D. Su¹⁴⁴, J. Su¹²⁶, R. Subramaniam⁸¹, S. Suchek^{60a}, Y. Sugaya¹¹⁹, M. Suk¹²⁹, V.V. Sulin⁹⁷, S. Sultansoy^{4c}, T. Sumida⁷⁰, S. Sun⁵⁹, X. Sun^{35a}, J.E. Sundermann⁵⁰, K. Suruliz¹⁵⁰, G. Susinno^{39a,39b}, M.R. Sutton¹⁵⁰, S. Suzuki⁶⁸, M. Svatos¹²⁸, M. Swiatlowski³³, I. Sykora^{145a}, T. Sykora¹³⁰, D. Ta⁵⁰, C. Taccini^{135a,135b}, K. Tackmann⁴⁴, J. Taenzer¹⁵⁹, A. Taffard¹⁶³, R. Tafirout^{160a}, N. Taiblum¹⁵⁴, H. Takai²⁷, R. Takashima⁷¹, T. Takeshita¹⁴¹, Y. Takubo⁶⁸, M. Talby⁸⁷, A.A. Talyshev^{110,c}, K.G. Tan⁹⁰, J. Tanaka¹⁵⁶, R. Tanaka¹¹⁸, S. Tanaka⁶⁸, B.B. Tannenwald¹¹², S. Tapia Araya^{34b}, S. Tapprogge⁸⁵, S. Tarem¹⁵³, G.F. Tartarelli^{93a}, P. Tas¹³⁰, M. Tasevsky¹²⁸, T. Tashiro⁷⁰, E. Tassi^{39a,39b}, A. Tavares Delgado^{127a,127b}, Y. Tayalati^{136d}, A.C. Taylor¹⁰⁶, G.N. Taylor⁹⁰, P.T.E. Taylor⁹⁰, W. Taylor^{160b}, F.A. Teischinger³², P. Teixeira-Dias⁷⁹, K.K. Temming⁵⁰, D. Temple¹⁴³, H. Ten Kate³², P.K. Teng¹⁵², J.J. Teoh¹¹⁹, F. Tepel¹⁷⁵, S. Terada⁶⁸, K. Terashi¹⁵⁶, J. Terron⁸⁴, S. Terzo¹⁰², M. Testa⁴⁹, R.J. Teuscher^{159,l}, T. Theveneaux-Pelzer⁸⁷, J.P. Thomas¹⁹, J. Thomas-Wilsker⁷⁹, E.N. Thompson³⁷, P.D. Thompson¹⁹, A.S. Thompson⁵⁵, L.A. Thomsen¹⁷⁶, E. Thomson¹²³, M. Thomson³⁰, M.J. Tibbetts¹⁶, R.E. Ticse Torres⁸⁷, V.O. Tikhomirov^{97,an}, Yu.A. Tikhonov^{110,c}, S. Timoshenko⁹⁹, P. Tipton¹⁷⁶, S. Tisserant⁸⁷, K. Todome¹⁵⁸, T. Todorov^{5,*}, S. Todorova-Nova¹³⁰, J. Tojo⁷², S. Tokár^{145a}, K. Tokushuku⁶⁸, E. Tolley⁵⁹, L. Tomlinson⁸⁶, M. Tomoto¹⁰⁴, L. Tompkins^{144,ao}, K. Toms¹⁰⁶, B. Tong⁵⁹, E. Torrence¹¹⁷, H. Torres¹⁴³, E. Torró Pastor¹³⁹, J. Toth^{87,ap}, F. Touchard⁸⁷, D.R. Tovey¹⁴⁰, T. Trefzger¹⁷⁴, A. Tricoli²⁷, I.M. Trigger^{160a}, S. Trincaz-Duvold⁸², M.F. Tripiana¹³, W. Trischuk¹⁵⁹, B. Trocmé⁵⁷, A. Trofymov⁴⁴, C. Troncon^{93a}, M. Trottier-McDonald¹⁶, M. Trovatelli¹⁶⁹, L. Truong^{164a,164c}, M. Trzebinski⁴¹, A. Trzupek⁴¹, J.C-L. Tseng¹²¹, P.V. Tsiareshka⁹⁴, G. Tsipolitis¹⁰, N. Tsirintanis⁹, S. Tsiskaridze¹³, V. Tsiskaridze⁵⁰, E.G. Tskhadadze^{53a}, K.M. Tsui^{62a}, I.I. Tsukerman⁹⁸, V. Tsulaia¹⁶, S. Tsuno⁶⁸, D. Tsybychev¹⁴⁹, A. Tudorache^{28b}, V. Tudorache^{28b}, A.N. Tuna⁵⁹, S.A. Tupputi^{22a,22b}, S. Turchikhin^{100,al}, D. Turecek¹²⁹, D. Turgeman¹⁷², R. Turra^{93a,93b}, A.J. Turvey⁴², P.M. Tuts³⁷, M. Tyndel¹³², G. Ucchielli^{22a,22b}, I. Ueda¹⁵⁶, R. Ueno³¹, M. Ughetto^{147a,147b}, F. Ukegawa¹⁶¹, G. Unal³², A. Undrus²⁷, G. Unel¹⁶³, F.C. Ungaro⁹⁰, Y. Unno⁶⁸, C. Unverdorben¹⁰¹, J. Urban^{145b}, P. Urquijo⁹⁰, P. Urrejola⁸⁵, G. Usai⁸, A. Usanova⁶⁴, L. Vacavant⁸⁷, V. Vacek¹²⁹, B. Vachon⁸⁹, C. Valderanis¹⁰¹, E. Valdes Santurio^{147a,147b}, N. Valencic¹⁰⁸, S. Valentinetto^{22a,22b},

A. Valero¹⁶⁷, L. Valery¹³, S. Valkar¹³⁰, S. Vallecorsa⁵¹, J.A. Valls Ferrer¹⁶⁷, W. Van Den Wollenberg¹⁰⁸, P.C. Van Der Deijl¹⁰⁸, R. van der Geer¹⁰⁸, H. van der Graaf¹⁰⁸, N. van Eldik¹⁵³, P. van Gemmeren⁶, J. Van Nieuwkoop¹⁴³, I. van Vulpen¹⁰⁸, M.C. van Woerden³², M. Vanadia^{133a,133b}, W. Vandelli³², R. Vanguri¹²³, A. Vaniachine¹³¹, P. Vankov¹⁰⁸, G. Vardanyan¹⁷⁷, R. Vari^{133a}, E.W. Varnes⁷, T. Varol⁴², D. Varouchas⁸², A. Vartapetian⁸, K.E. Varvell¹⁵¹, J.G. Vasquez¹⁷⁶, F. Vazeille³⁶, T. Vazquez Schroeder⁸⁹, J. Veatch⁵⁶, L.M. Veloce¹⁵⁹, F. Veloso^{127a,127c}, S. Veneziano^{133a}, A. Ventura^{75a,75b}, M. Venturi¹⁶⁹, N. Venturi¹⁵⁹, A. Venturini²⁵, V. Vercesi^{122a}, M. Verducci^{133a,133b}, W. Verkerke¹⁰⁸, J.C. Vermeulen¹⁰⁸, A. Vest^{46,aq}, M.C. Vetterli^{143,d}, O. Viazlo⁸³, I. Vichou¹⁶⁶, T. Vickey¹⁴⁰, O.E. Vickey Boeriu¹⁴⁰, G.H.A. Viehhauser¹²¹, S. Viel¹⁶, L. Vigani¹²¹, R. Vigne⁶⁴, M. Villa^{22a,22b}, M. Villaplana Perez^{93a,93b}, E. Vilucchi⁴⁹, M.G. Vincter³¹, V.B. Vinogradov⁶⁷, C. Vittori^{22a,22b}, I. Vivarelli¹⁵⁰, S. Vlachos¹⁰, M. Vlasak¹²⁹, M. Vogel¹⁷⁵, P. Vokac¹²⁹, G. Volpi^{125a,125b}, M. Volpi⁹⁰, H. von der Schmitt¹⁰², E. von Toerne²³, V. Vorobel¹³⁰, K. Vorobej⁹⁹, M. Vos¹⁶⁷, R. Voss³², J.H. Vossebeld⁷⁶, N. Vranjes¹⁴, M. Vranjes Milosavljevic¹⁴, V. Vrba¹²⁸, M. Vreeswijk¹⁰⁸, R. Vuillermet³², I. Vukotic³³, Z. Vykydal¹²⁹, P. Wagner²³, W. Wagner¹⁷⁵, H. Wahlberg⁷³, S. Wahr mund⁴⁶, J. Wakabayashi¹⁰⁴, J. Walder⁷⁴, R. Walker¹⁰¹, W. Walkowiak¹⁴², V. Wallangen^{147a,147b}, C. Wang^{35c}, C. Wang^{35d,87}, F. Wang¹⁷³, H. Wang¹⁶, H. Wang⁴², J. Wang⁴⁴, J. Wang¹⁵¹, K. Wang⁸⁹, R. Wang⁶, S.M. Wang¹⁵², T. Wang²³, T. Wang³⁷, W. Wang^{35b}, X. Wang¹⁷⁶, C. Wanotayaroj¹¹⁷, A. Warburton⁸⁹, C.P. Ward³⁰, D.R. Wardrop⁸⁰, A. Washbrook⁴⁸, P.M. Watkins¹⁹, A.T. Watson¹⁹, M.F. Watson¹⁹, G. Watts¹³⁹, S. Watts⁸⁶, B.M. Waugh⁸⁰, S. Webb⁸⁵, M.S. Weber¹⁸, S.W. Weber¹⁷⁴, J.S. Webster⁶, A.R. Weidberg¹²¹, B. Weinert⁶³, J. Weingarten⁵⁶, C. Weiser⁵⁰, H. Weits¹⁰⁸, P.S. Wells³², T. Wenaus²⁷, T. Wengler³², S. Wenig³², N. Wermes²³, M. Werner⁵⁰, M.D. Werner⁶⁶, P. Werner³², M. Wessels^{60a}, J. Wetter¹⁶², K. Whalen¹¹⁷, N.L. Whallon¹³⁹, A.M. Wharton⁷⁴, A. White⁸, M.J. White¹, R. White^{34b}, D. Whiteson¹⁶³, F.J. Wickens¹³², W. Wiedenmann¹⁷³, M. Wielers¹³², P. Wienemann²³, C. Wiglesworth³⁸, L.A.M. Wiik-Fuchs²³, A. Wildauer¹⁰², F. Wilk⁸⁶, H.G. Wilkens³², H.H. Williams¹²³, S. Williams¹⁰⁸, C. Willis⁹², S. Willocq⁸⁸, J.A. Wilson¹⁹, I. Wingerter-Seez⁵, F. Winklmeier¹¹⁷, O.J. Winston¹⁵⁰, B.T. Winter²³, M. Wittgen¹⁴⁴, J. Wittkowski¹⁰¹, S.J. Wollstadt⁸⁵, M.W. Wolter⁴¹, H. Wolters^{127a,127c}, B.K. Wosiek⁴¹, J. Wotschack³², M.J. Woudstra⁸⁶, K.W. Wozniak⁴¹, M. Wu⁵⁷, M. Wu³³, S.L. Wu¹⁷³, X. Wu⁵¹, Y. Wu⁹¹, T.R. Wyatt⁸⁶, B.M. Wynne⁴⁸, S. Xella³⁸, D. Xu^{35a}, L. Xu²⁷, B. Yabsley¹⁵¹, S. Yacoob^{146a}, R. Yakabe⁶⁹, D. Yamaguchi¹⁵⁸, Y. Yamaguchi¹¹⁹, A. Yamamoto⁶⁸, S. Yamamoto¹⁵⁶, T. Yamanaka¹⁵⁶, K. Yamauchi¹⁰⁴, Y. Yamazaki⁶⁹, Z. Yan²⁴, H. Yang^{35e}, H. Yang¹⁷³, Y. Yang¹⁵², Z. Yang¹⁵, W-M. Yao¹⁶, Y.C. Yap⁸², Y. Yasu⁶⁸, E. Yatsenko⁵, K.H. Yau Wong²³, J. Ye⁴², S. Ye²⁷, I. Yeletskikh⁶⁷, A.L. Yen⁵⁹, E. Yildirim⁸⁵, K. Yorita¹⁷¹, R. Yoshida⁶, K. Yoshihara¹²³, C. Young¹⁴⁴, C.J.S. Young³², S. Youssef²⁴, D.R. Yu¹⁶, J. Yu⁸, J.M. Yu⁹¹, J. Yu⁶⁶, L. Yuan⁶⁹, S.P.Y. Yuen²³, I. Yusuff^{30,ar}, B. Zabinski⁴¹, R. Zaidan^{35d}, A.M. Zaitsev^{131,ae}, N. Zakharchuk⁴⁴, J. Zalieckas¹⁵, A. Zaman¹⁴⁹, S. Zambito⁵⁹, L. Zanello^{133a,133b}, D. Zanzi⁹⁰, C. Zeitnitz¹⁷⁵, M. Zeman¹²⁹, A. Zemla^{40a}, J.C. Zeng¹⁶⁶, Q. Zeng¹⁴⁴, K. Zengel²⁵, O. Zenin¹³¹, T. Ženiš^{145a}, D. Zerwas¹¹⁸, D. Zhang⁹¹, F. Zhang¹⁷³, G. Zhang^{35b,am}, H. Zhang^{35c}, J. Zhang⁶, L. Zhang⁵⁰, R. Zhang²³, R. Zhang^{35b,as}, X. Zhang^{35d}, Z. Zhang¹¹⁸, X. Zhao⁴², Y. Zhao^{35d}, Z. Zhao^{35b}, A. Zhemchugov⁶⁷, J. Zhong¹²¹, B. Zhou⁹¹, C. Zhou⁴⁷, L. Zhou³⁷, L. Zhou⁴², M. Zhou¹⁴⁹, N. Zhou^{35f}, C.G. Zhu^{35d}, H. Zhu^{35a}, J. Zhu⁹¹, Y. Zhu^{35b}, X. Zhuang^{35a}, K. Zhukov⁹⁷, A. Zibell¹⁷⁴, D. Ziemińska⁶³, N.I. Zimine⁶⁷, C. Zimmermann⁸⁵, S. Zimmermann⁵⁰, Z. Zinonos⁵⁶, M. Zinser⁸⁵, M. Ziolkowski¹⁴², L. Živković¹⁴, G. Zobernig¹⁷³, A. Zoccoli^{22a,22b}, M. zur Nedden¹⁷, G. Zurzolo^{105a,105b}, L. Zwalski³².

¹ Department of Physics, University of Adelaide, Adelaide, Australia

² Physics Department, SUNY Albany, Albany NY, United States of America

³ Department of Physics, University of Alberta, Edmonton AB, Canada

⁴ ^(a) Department of Physics, Ankara University, Ankara; ^(b) Istanbul Aydin University, Istanbul; ^(c)

- Division of Physics, TOBB University of Economics and Technology, Ankara, Turkey
- ⁵ LAPP, CNRS/IN2P3 and Université Savoie Mont Blanc, Annecy-le-Vieux, France
- ⁶ High Energy Physics Division, Argonne National Laboratory, Argonne IL, United States of America
- ⁷ Department of Physics, University of Arizona, Tucson AZ, United States of America
- ⁸ Department of Physics, The University of Texas at Arlington, Arlington TX, United States of America
- ⁹ Physics Department, University of Athens, Athens, Greece
- ¹⁰ Physics Department, National Technical University of Athens, Zografou, Greece
- ¹¹ Department of Physics, The University of Texas at Austin, Austin TX, United States of America
- ¹² Institute of Physics, Azerbaijan Academy of Sciences, Baku, Azerbaijan
- ¹³ Institut de Física d'Altes Energies (IFAE), The Barcelona Institute of Science and Technology, Barcelona, Spain, Spain
- ¹⁴ Institute of Physics, University of Belgrade, Belgrade, Serbia
- ¹⁵ Department for Physics and Technology, University of Bergen, Bergen, Norway
- ¹⁶ Physics Division, Lawrence Berkeley National Laboratory and University of California, Berkeley CA, United States of America
- ¹⁷ Department of Physics, Humboldt University, Berlin, Germany
- ¹⁸ Albert Einstein Center for Fundamental Physics and Laboratory for High Energy Physics, University of Bern, Bern, Switzerland
- ¹⁹ School of Physics and Astronomy, University of Birmingham, Birmingham, United Kingdom
- ²⁰ ^(a) Department of Physics, Bogazici University, Istanbul; ^(b) Department of Physics Engineering, Gaziantep University, Gaziantep; ^(d) Istanbul Bilgi University, Faculty of Engineering and Natural Sciences, Istanbul, Turkey; ^(e) Bahcesehir University, Faculty of Engineering and Natural Sciences, Istanbul, Turkey, Turkey
- ²¹ Centro de Investigaciones, Universidad Antonio Narino, Bogota, Colombia
- ²² ^(a) INFN Sezione di Bologna; ^(b) Dipartimento di Fisica e Astronomia, Università di Bologna, Bologna, Italy
- ²³ Physikalisches Institut, University of Bonn, Bonn, Germany
- ²⁴ Department of Physics, Boston University, Boston MA, United States of America
- ²⁵ Department of Physics, Brandeis University, Waltham MA, United States of America
- ²⁶ ^(a) Universidade Federal do Rio De Janeiro COPPE/EE/IF, Rio de Janeiro; ^(b) Electrical Circuits Department, Federal University of Juiz de Fora (UFJF), Juiz de Fora; ^(c) Federal University of Sao Joao del Rei (UFSJ), Sao Joao del Rei; ^(d) Instituto de Fisica, Universidade de Sao Paulo, Sao Paulo, Brazil
- ²⁷ Physics Department, Brookhaven National Laboratory, Upton NY, United States of America
- ²⁸ ^(a) Transilvania University of Brasov, Brasov, Romania; ^(b) National Institute of Physics and Nuclear Engineering, Bucharest; ^(c) National Institute for Research and Development of Isotopic and Molecular Technologies, Physics Department, Cluj Napoca; ^(d) University Politehnica Bucharest, Bucharest; ^(e) West University in Timisoara, Timisoara, Romania
- ²⁹ Departamento de Física, Universidad de Buenos Aires, Buenos Aires, Argentina
- ³⁰ Cavendish Laboratory, University of Cambridge, Cambridge, United Kingdom
- ³¹ Department of Physics, Carleton University, Ottawa ON, Canada
- ³² CERN, Geneva, Switzerland
- ³³ Enrico Fermi Institute, University of Chicago, Chicago IL, United States of America
- ³⁴ ^(a) Departamento de Física, Pontificia Universidad Católica de Chile, Santiago; ^(b) Departamento de Física, Universidad Técnica Federico Santa María, Valparaíso, Chile
- ³⁵ ^(a) Institute of High Energy Physics, Chinese Academy of Sciences, Beijing; ^(b) Department of Modern Physics, University of Science and Technology of China, Anhui; ^(c) Department of Physics, Nanjing University, Jiangsu; ^(d) School of Physics, Shandong University, Shandong; ^(e) Department of

Physics and Astronomy, Shanghai Key Laboratory for Particle Physics and Cosmology, Shanghai Jiao Tong University, Shanghai; (also affiliated with PKU-CHEP); ^(f) Physics Department, Tsinghua University, Beijing 100084, China

³⁶ Laboratoire de Physique Corpusculaire, Clermont Université and Université Blaise Pascal and CNRS/IN2P3, Clermont-Ferrand, France

³⁷ Nevis Laboratory, Columbia University, Irvington NY, United States of America

³⁸ Niels Bohr Institute, University of Copenhagen, Kobenhavn, Denmark

³⁹ ^(a) INFN Gruppo Collegato di Cosenza, Laboratori Nazionali di Frascati; ^(b) Dipartimento di Fisica, Università della Calabria, Rende, Italy

⁴⁰ ^(a) AGH University of Science and Technology, Faculty of Physics and Applied Computer Science, Krakow; ^(b) Marian Smoluchowski Institute of Physics, Jagiellonian University, Krakow, Poland

⁴¹ Institute of Nuclear Physics Polish Academy of Sciences, Krakow, Poland

⁴² Physics Department, Southern Methodist University, Dallas TX, United States of America

⁴³ Physics Department, University of Texas at Dallas, Richardson TX, United States of America

⁴⁴ DESY, Hamburg and Zeuthen, Germany

⁴⁵ Institut für Experimentelle Physik IV, Technische Universität Dortmund, Dortmund, Germany

⁴⁶ Institut für Kern- und Teilchenphysik, Technische Universität Dresden, Dresden, Germany

⁴⁷ Department of Physics, Duke University, Durham NC, United States of America

⁴⁸ SUPA - School of Physics and Astronomy, University of Edinburgh, Edinburgh, United Kingdom

⁴⁹ INFN Laboratori Nazionali di Frascati, Frascati, Italy

⁵⁰ Fakultät für Mathematik und Physik, Albert-Ludwigs-Universität, Freiburg, Germany

⁵¹ Section de Physique, Université de Genève, Geneva, Switzerland

⁵² ^(a) INFN Sezione di Genova; ^(b) Dipartimento di Fisica, Università di Genova, Genova, Italy

⁵³ ^(a) E. Andronikashvili Institute of Physics, Iv. Javakhishvili Tbilisi State University, Tbilisi; ^(b) High Energy Physics Institute, Tbilisi State University, Tbilisi, Georgia

⁵⁴ II Physikalisches Institut, Justus-Liebig-Universität Giessen, Giessen, Germany

⁵⁵ SUPA - School of Physics and Astronomy, University of Glasgow, Glasgow, United Kingdom

⁵⁶ II Physikalisches Institut, Georg-August-Universität, Göttingen, Germany

⁵⁷ Laboratoire de Physique Subatomique et de Cosmologie, Université Grenoble-Alpes, CNRS/IN2P3, Grenoble, France

⁵⁸ Department of Physics, Hampton University, Hampton VA, United States of America

⁵⁹ Laboratory for Particle Physics and Cosmology, Harvard University, Cambridge MA, United States of America

⁶⁰ ^(a) Kirchhoff-Institut für Physik, Ruprecht-Karls-Universität Heidelberg, Heidelberg; ^(b) Physikalisches Institut, Ruprecht-Karls-Universität Heidelberg, Heidelberg; ^(c) ZITI Institut für technische Informatik, Ruprecht-Karls-Universität Heidelberg, Mannheim, Germany

⁶¹ Faculty of Applied Information Science, Hiroshima Institute of Technology, Hiroshima, Japan

⁶² ^(a) Department of Physics, The Chinese University of Hong Kong, Shatin, N.T., Hong Kong; ^(b) Department of Physics, The University of Hong Kong, Hong Kong; ^(c) Department of Physics, The Hong Kong University of Science and Technology, Clear Water Bay, Kowloon, Hong Kong, China

⁶³ Department of Physics, Indiana University, Bloomington IN, United States of America

⁶⁴ Institut für Astro- und Teilchenphysik, Leopold-Franzens-Universität, Innsbruck, Austria

⁶⁵ University of Iowa, Iowa City IA, United States of America

⁶⁶ Department of Physics and Astronomy, Iowa State University, Ames IA, United States of America

⁶⁷ Joint Institute for Nuclear Research, JINR Dubna, Dubna, Russia

⁶⁸ KEK, High Energy Accelerator Research Organization, Tsukuba, Japan

⁶⁹ Graduate School of Science, Kobe University, Kobe, Japan

- ⁷⁰ Faculty of Science, Kyoto University, Kyoto, Japan
⁷¹ Kyoto University of Education, Kyoto, Japan
⁷² Department of Physics, Kyushu University, Fukuoka, Japan
⁷³ Instituto de Física La Plata, Universidad Nacional de La Plata and CONICET, La Plata, Argentina
⁷⁴ Physics Department, Lancaster University, Lancaster, United Kingdom
⁷⁵ ^(a) INFN Sezione di Lecce; ^(b) Dipartimento di Matematica e Fisica, Università del Salento, Lecce, Italy
⁷⁶ Oliver Lodge Laboratory, University of Liverpool, Liverpool, United Kingdom
⁷⁷ Department of Physics, Jožef Stefan Institute and University of Ljubljana, Ljubljana, Slovenia
⁷⁸ School of Physics and Astronomy, Queen Mary University of London, London, United Kingdom
⁷⁹ Department of Physics, Royal Holloway University of London, Surrey, United Kingdom
⁸⁰ Department of Physics and Astronomy, University College London, London, United Kingdom
⁸¹ Louisiana Tech University, Ruston LA, United States of America
⁸² Laboratoire de Physique Nucléaire et de Hautes Energies, UPMC and Université Paris-Diderot and CNRS/IN2P3, Paris, France
⁸³ Fysiska institutionen, Lunds universitet, Lund, Sweden
⁸⁴ Departamento de Fisica Teorica C-15, Universidad Autonoma de Madrid, Madrid, Spain
⁸⁵ Institut für Physik, Universität Mainz, Mainz, Germany
⁸⁶ School of Physics and Astronomy, University of Manchester, Manchester, United Kingdom
⁸⁷ CPPM, Aix-Marseille Université and CNRS/IN2P3, Marseille, France
⁸⁸ Department of Physics, University of Massachusetts, Amherst MA, United States of America
⁸⁹ Department of Physics, McGill University, Montreal QC, Canada
⁹⁰ School of Physics, University of Melbourne, Victoria, Australia
⁹¹ Department of Physics, The University of Michigan, Ann Arbor MI, United States of America
⁹² Department of Physics and Astronomy, Michigan State University, East Lansing MI, United States of America
⁹³ ^(a) INFN Sezione di Milano; ^(b) Dipartimento di Fisica, Università di Milano, Milano, Italy
⁹⁴ B.I. Stepanov Institute of Physics, National Academy of Sciences of Belarus, Minsk, Republic of Belarus
⁹⁵ National Scientific and Educational Centre for Particle and High Energy Physics, Minsk, Republic of Belarus
⁹⁶ Group of Particle Physics, University of Montreal, Montreal QC, Canada
⁹⁷ P.N. Lebedev Physical Institute of the Russian Academy of Sciences, Moscow, Russia
⁹⁸ Institute for Theoretical and Experimental Physics (ITEP), Moscow, Russia
⁹⁹ National Research Nuclear University MEPhI, Moscow, Russia
¹⁰⁰ D.V. Skobeltsyn Institute of Nuclear Physics, M.V. Lomonosov Moscow State University, Moscow, Russia
¹⁰¹ Fakultät für Physik, Ludwig-Maximilians-Universität München, München, Germany
¹⁰² Max-Planck-Institut für Physik (Werner-Heisenberg-Institut), München, Germany
¹⁰³ Nagasaki Institute of Applied Science, Nagasaki, Japan
¹⁰⁴ Graduate School of Science and Kobayashi-Maskawa Institute, Nagoya University, Nagoya, Japan
¹⁰⁵ ^(a) INFN Sezione di Napoli; ^(b) Dipartimento di Fisica, Università di Napoli, Napoli, Italy
¹⁰⁶ Department of Physics and Astronomy, University of New Mexico, Albuquerque NM, United States of America
¹⁰⁷ Institute for Mathematics, Astrophysics and Particle Physics, Radboud University Nijmegen/Nikhef, Nijmegen, Netherlands
¹⁰⁸ Nikhef National Institute for Subatomic Physics and University of Amsterdam, Amsterdam,

Netherlands

¹⁰⁹ Department of Physics, Northern Illinois University, DeKalb IL, United States of America

¹¹⁰ Budker Institute of Nuclear Physics, SB RAS, Novosibirsk, Russia

¹¹¹ Department of Physics, New York University, New York NY, United States of America

¹¹² Ohio State University, Columbus OH, United States of America

¹¹³ Faculty of Science, Okayama University, Okayama, Japan

¹¹⁴ Homer L. Dodge Department of Physics and Astronomy, University of Oklahoma, Norman OK, United States of America

¹¹⁵ Department of Physics, Oklahoma State University, Stillwater OK, United States of America

¹¹⁶ Palacký University, RCPTM, Olomouc, Czech Republic

¹¹⁷ Center for High Energy Physics, University of Oregon, Eugene OR, United States of America

¹¹⁸ LAL, Univ. Paris-Sud, CNRS/IN2P3, Université Paris-Saclay, Orsay, France

¹¹⁹ Graduate School of Science, Osaka University, Osaka, Japan

¹²⁰ Department of Physics, University of Oslo, Oslo, Norway

¹²¹ Department of Physics, Oxford University, Oxford, United Kingdom

¹²² ^(a) INFN Sezione di Pavia; ^(b) Dipartimento di Fisica, Università di Pavia, Pavia, Italy

¹²³ Department of Physics, University of Pennsylvania, Philadelphia PA, United States of America

¹²⁴ National Research Centre "Kurchatov Institute" B.P.Konstantinov Petersburg Nuclear Physics Institute, St. Petersburg, Russia

¹²⁵ ^(a) INFN Sezione di Pisa; ^(b) Dipartimento di Fisica E. Fermi, Università di Pisa, Pisa, Italy

¹²⁶ Department of Physics and Astronomy, University of Pittsburgh, Pittsburgh PA, United States of America

¹²⁷ ^(a) Laboratório de Instrumentação e Física Experimental de Partículas - LIP, Lisboa; ^(b) Faculdade de Ciências, Universidade de Lisboa, Lisboa; ^(c) Department of Physics, University of Coimbra, Coimbra; ^(d) Centro de Física Nuclear da Universidade de Lisboa, Lisboa; ^(e) Departamento de Fisica, Universidade do Minho, Braga; ^(f) Departamento de Fisica Teorica y del Cosmos and CAFPE, Universidad de Granada, Granada (Spain); ^(g) Dep Fisica and CEFITEC of Faculdade de Ciencias e Tecnologia, Universidade Nova de Lisboa, Caparica, Portugal

¹²⁸ Institute of Physics, Academy of Sciences of the Czech Republic, Praha, Czech Republic

¹²⁹ Czech Technical University in Prague, Praha, Czech Republic

¹³⁰ Faculty of Mathematics and Physics, Charles University in Prague, Praha, Czech Republic

¹³¹ State Research Center Institute for High Energy Physics (Protvino), NRC KI, Russia

¹³² Particle Physics Department, Rutherford Appleton Laboratory, Didcot, United Kingdom

¹³³ ^(a) INFN Sezione di Roma; ^(b) Dipartimento di Fisica, Sapienza Università di Roma, Roma, Italy

¹³⁴ ^(a) INFN Sezione di Roma Tor Vergata; ^(b) Dipartimento di Fisica, Università di Roma Tor Vergata, Roma, Italy

¹³⁵ ^(a) INFN Sezione di Roma Tre; ^(b) Dipartimento di Matematica e Fisica, Università Roma Tre, Roma, Italy

¹³⁶ ^(a) Faculté des Sciences Ain Chock, Réseau Universitaire de Physique des Hautes Energies - Université Hassan II, Casablanca; ^(b) Centre National de l'Energie des Sciences Techniques Nucléaires, Rabat; ^(c) Faculté des Sciences Semlalia, Université Cadi Ayyad, LPHEA-Marrakech; ^(d) Faculté des Sciences, Université Mohamed Premier and LPTPM, Oujda; ^(e) Faculté des sciences, Université Mohammed V, Rabat, Morocco

¹³⁷ DSM/IRFU (Institut de Recherches sur les Lois Fondamentales de l'Univers), CEA Saclay (Commissariat à l'Energie Atomique et aux Energies Alternatives), Gif-sur-Yvette, France

¹³⁸ Santa Cruz Institute for Particle Physics, University of California Santa Cruz, Santa Cruz CA, United States of America

- ¹³⁹ Department of Physics, University of Washington, Seattle WA, United States of America
¹⁴⁰ Department of Physics and Astronomy, University of Sheffield, Sheffield, United Kingdom
¹⁴¹ Department of Physics, Shinshu University, Nagano, Japan
¹⁴² Fachbereich Physik, Universität Siegen, Siegen, Germany
¹⁴³ Department of Physics, Simon Fraser University, Burnaby BC, Canada
¹⁴⁴ SLAC National Accelerator Laboratory, Stanford CA, United States of America
¹⁴⁵ ^(a) Faculty of Mathematics, Physics & Informatics, Comenius University, Bratislava; ^(b) Department of Subnuclear Physics, Institute of Experimental Physics of the Slovak Academy of Sciences, Kosice, Slovak Republic
¹⁴⁶ ^(a) Department of Physics, University of Cape Town, Cape Town; ^(b) Department of Physics, University of Johannesburg, Johannesburg; ^(c) School of Physics, University of the Witwatersrand, Johannesburg, South Africa
¹⁴⁷ ^(a) Department of Physics, Stockholm University; ^(b) The Oskar Klein Centre, Stockholm, Sweden
¹⁴⁸ Physics Department, Royal Institute of Technology, Stockholm, Sweden
¹⁴⁹ Departments of Physics & Astronomy and Chemistry, Stony Brook University, Stony Brook NY, United States of America
¹⁵⁰ Department of Physics and Astronomy, University of Sussex, Brighton, United Kingdom
¹⁵¹ School of Physics, University of Sydney, Sydney, Australia
¹⁵² Institute of Physics, Academia Sinica, Taipei, Taiwan
¹⁵³ Department of Physics, Technion: Israel Institute of Technology, Haifa, Israel
¹⁵⁴ Raymond and Beverly Sackler School of Physics and Astronomy, Tel Aviv University, Tel Aviv, Israel
¹⁵⁵ Department of Physics, Aristotle University of Thessaloniki, Thessaloniki, Greece
¹⁵⁶ International Center for Elementary Particle Physics and Department of Physics, The University of Tokyo, Tokyo, Japan
¹⁵⁷ Graduate School of Science and Technology, Tokyo Metropolitan University, Tokyo, Japan
¹⁵⁸ Department of Physics, Tokyo Institute of Technology, Tokyo, Japan
¹⁵⁹ Department of Physics, University of Toronto, Toronto ON, Canada
¹⁶⁰ ^(a) TRIUMF, Vancouver BC; ^(b) Department of Physics and Astronomy, York University, Toronto ON, Canada
¹⁶¹ Faculty of Pure and Applied Sciences, and Center for Integrated Research in Fundamental Science and Engineering, University of Tsukuba, Tsukuba, Japan
¹⁶² Department of Physics and Astronomy, Tufts University, Medford MA, United States of America
¹⁶³ Department of Physics and Astronomy, University of California Irvine, Irvine CA, United States of America
¹⁶⁴ ^(a) INFN Gruppo Collegato di Udine, Sezione di Trieste, Udine; ^(b) ICTP, Trieste; ^(c) Dipartimento di Chimica, Fisica e Ambiente, Università di Udine, Udine, Italy
¹⁶⁵ Department of Physics and Astronomy, University of Uppsala, Uppsala, Sweden
¹⁶⁶ Department of Physics, University of Illinois, Urbana IL, United States of America
¹⁶⁷ Instituto de Física Corpuscular (IFIC) and Departamento de Física Atomica, Molecular y Nuclear and Departamento de Ingeniería Electrónica and Instituto de Microelectrónica de Barcelona (IMB-CNM), University of Valencia and CSIC, Valencia, Spain
¹⁶⁸ Department of Physics, University of British Columbia, Vancouver BC, Canada
¹⁶⁹ Department of Physics and Astronomy, University of Victoria, Victoria BC, Canada
¹⁷⁰ Department of Physics, University of Warwick, Coventry, United Kingdom
¹⁷¹ Waseda University, Tokyo, Japan
¹⁷² Department of Particle Physics, The Weizmann Institute of Science, Rehovot, Israel

- ¹⁷³ Department of Physics, University of Wisconsin, Madison WI, United States of America
¹⁷⁴ Fakultät für Physik und Astronomie, Julius-Maximilians-Universität, Würzburg, Germany
¹⁷⁵ Fakultät für Mathematik und Naturwissenschaften, Fachgruppe Physik, Bergische Universität Wuppertal, Wuppertal, Germany
¹⁷⁶ Department of Physics, Yale University, New Haven CT, United States of America
¹⁷⁷ Yerevan Physics Institute, Yerevan, Armenia
¹⁷⁸ Centre de Calcul de l’Institut National de Physique Nucléaire et de Physique des Particules (IN2P3), Villeurbanne, France
^a Also at Department of Physics, King’s College London, London, United Kingdom
^b Also at Institute of Physics, Azerbaijan Academy of Sciences, Baku, Azerbaijan
^c Also at Novosibirsk State University, Novosibirsk, Russia
^d Also at TRIUMF, Vancouver BC, Canada
^e Also at Department of Physics & Astronomy, University of Louisville, Louisville, KY, United States of America
^f Also at Department of Physics, California State University, Fresno CA, United States of America
^g Also at Department of Physics, University of Fribourg, Fribourg, Switzerland
^h Also at Departament de Fisica de la Universitat Autonoma de Barcelona, Barcelona, Spain
ⁱ Also at Departamento de Fisica e Astronomia, Faculdade de Ciencias, Universidade do Porto, Portugal
^j Also at Tomsk State University, Tomsk, Russia
^k Also at Universita di Napoli Parthenope, Napoli, Italy
^l Also at Institute of Particle Physics (IPP), Canada
^m Also at National Institute of Physics and Nuclear Engineering, Bucharest, Romania
ⁿ Also at Department of Physics, St. Petersburg State Polytechnical University, St. Petersburg, Russia
^o Also at Department of Physics, The University of Michigan, Ann Arbor MI, United States of America
^p Also at Centre for High Performance Computing, CSIR Campus, Rosebank, Cape Town, South Africa
^q Also at Louisiana Tech University, Ruston LA, United States of America
^r Also at Institutio Catalana de Recerca i Estudis Avancats, ICREA, Barcelona, Spain
^s Also at Graduate School of Science, Osaka University, Osaka, Japan
^t Also at Department of Physics, National Tsing Hua University, Taiwan
^u Also at Institute for Mathematics, Astrophysics and Particle Physics, Radboud University Nijmegen/Nikhef, Nijmegen, Netherlands
^v Also at Department of Physics, The University of Texas at Austin, Austin TX, United States of America
^w Also at Institute of Theoretical Physics, Ilia State University, Tbilisi, Georgia
^x Also at CERN, Geneva, Switzerland
^y Also at Georgian Technical University (GTU), Tbilisi, Georgia
^z Also at Ochadai Academic Production, Ochanomizu University, Tokyo, Japan
^{aa} Also at Manhattan College, New York NY, United States of America
^{ab} Also at Hellenic Open University, Patras, Greece
^{ac} Also at Academia Sinica Grid Computing, Institute of Physics, Academia Sinica, Taipei, Taiwan
^{ad} Also at School of Physics, Shandong University, Shandong, China
^{ae} Also at Moscow Institute of Physics and Technology State University, Dolgoprudny, Russia
^{af} Also at Section de Physique, Université de Genève, Geneva, Switzerland
^{ag} Also at Eotvos Lorand University, Budapest, Hungary
^{ah} Also at International School for Advanced Studies (SISSA), Trieste, Italy
^{ai} Also at Department of Physics and Astronomy, University of South Carolina, Columbia SC, United States of America
^{aj} Also at School of Physics and Engineering, Sun Yat-sen University, Guangzhou, China

ak Also at Institute for Nuclear Research and Nuclear Energy (INRNE) of the Bulgarian Academy of Sciences, Sofia, Bulgaria

al Also at Faculty of Physics, M.V.Lomonosov Moscow State University, Moscow, Russia

am Also at Institute of Physics, Academia Sinica, Taipei, Taiwan

an Also at National Research Nuclear University MEPhI, Moscow, Russia

ao Also at Department of Physics, Stanford University, Stanford CA, United States of America

ap Also at Institute for Particle and Nuclear Physics, Wigner Research Centre for Physics, Budapest, Hungary

aq Also at Flensburg University of Applied Sciences, Flensburg, Germany

ar Also at University of Malaya, Department of Physics, Kuala Lumpur, Malaysia

as Also at CPPM, Aix-Marseille Université and CNRS/IN2P3, Marseille, France

* Deceased